Stem Cell Reports
Article

ISSCR

OPEN ACCESS

An Expandable, Inducible Hemangioblast State Regulated by Fibroblast Growth Factor

David T. Vereide,[1,2,*] Vernella Vickerman,[1] Scott A. Swanson,[1] Li-Fang Chu,[1] Brian E. McIntosh,[1] and James A. Thomson[1,3,4,*]

[1]Morgridge Institute for Research, Madison, WI 53715, USA
[2]Biotechnology Center, University of Wisconsin-Madison, Madison, WI 53706, USA
[3]Department of Cell and Regenerative Biology, University of Wisconsin School of Medicine and Public Health, Madison, WI 53705, USA
[4]Department of Molecular, Cellular, and Developmental Biology, University of California, Santa Barbara, Santa Barbara, CA 93106, USA
*Correspondence: dvereide@morgridge.org (D.T.V.), jthomson@morgridge.org (J.A.T.)
http://dx.doi.org/10.1016/j.stemcr.2014.10.003

SUMMARY

During development, the hematopoietic and vascular lineages are thought to descend from common mesodermal progenitors called hemangioblasts. Here we identify six transcription factors, *Gata2*, *Lmo2*, *Mycn*, *Pitx2*, *Sox17*, and *Tal1*, that "trap" murine cells in a proliferative state and endow them with a hemangioblast potential. These "expandable" hemangioblasts (eHBs) are capable, once released from the control of the ectopic factors, to give rise to functional endothelial cells, multilineage hematopoietic cells, and smooth muscle cells. The eHBs can be derived from embryonic stem cells, from fetal liver cells, or poorly from fibroblasts. The eHBs reveal a central role for fibroblast growth factor, which not only promotes their expansion, but also facilitates their ability to give rise to endothelial cells and leukocytes, but not erythrocytes. This study serves as a demonstration that ephemeral progenitor states can be harnessed in vitro, enabling the creation of tractable progenitor cell lines.

INTRODUCTION

In developing mammals, hematopoiesis initially occurs extraembryonically, most prominently in the yolk sac (Silver and Palis, 1997), and later arises within the embryo in the aorta-gonad-mesonephros (AGM) region (Godin et al., 1993; Medvinsky et al., 1993) and developing endocardium (Nakano et al., 2013). Definitive hematopoietic stem cells (HSCs), which are responsible for blood production throughout life, first detectibly emerge in the AGM (Müller et al., 1994) and colonize the fetal liver (FL), ultimately occupying niches in the bone marrow (reviewed in Mikkola and Orkin, 2006). The specification of blood is closely coordinated with the specification of blood vessels, and genetic evidence supports the notion of a shared ontogeny. For example, murine embryos null for *Kdr* (also known as *Flk1*) do not develop blood islands or blood vessels and die between embryonic development days 8.5 and 9.5 (Shalaby et al., 1995). In chimeric embryos, *Kdr* null cells are not detected in later sites of hematopoiesis such as the FL or adult bone marrow but are found in other mesodermal tissues like heart, kidney, and muscle (Shalaby et al., 1997). In fact, endothelial cells and hematopoietic cells can be observed in vitro to arise from the same mesodermal progenitors, called hemangioblasts (Choi et al., 1998).

Previously, our group has isolated human embryonic stem cells (ESCs) whose pluripotent state is maintained in vitro by exogenous growth factor signaling, particularly fibroblast growth factor (FGF), insulin or insulin-like growth factor, and transforming growth factor (Bendall et al., 2007; Chen et al., 2011; Thomson et al., 1998; Vallier et al., 2005; Wang et al., 2007; Xu et al., 2005). These ESCs, in contrast to their ephemeral progenitor counterparts in vivo, can be cultured for many generations in the pluripotent state—they are fortuitously "trapped" in this state by the exogenous growth factor signaling, which sustains the expression of master transcription factors, including *POU5F1*, *SOX2*, and *NANOG*. These same factors, when ectopically expressed, can induce somatic cells to adopt a pluripotent stem (iPS) state (Takahashi et al., 2007; Takahashi and Yamanaka, 2006; Yu et al., 2007). Once iPS cells are reprogrammed, the ectopic factors are no longer required, as the endogenous factors can be maintained by the appropriate exogenous growth factor signaling.

A concept that thus emerges from these studies is that a core set of factors is central to both the induction and maintenance of a particular cell state. There are now numerous examples of inducing a desired cell state by the ectopic expression of key factors (reviewed in Pereira et al., 2012), for example, reprogramming fibroblasts to cells with characteristics of cardiomyocytes or hemogenic endothelium (Ieda et al., 2010; Pereira et al., 2013). In this study, we did not set out to reprogram cells per se; rather, we set out to determine the feasibility of employing core factors to maintain progenitors in culture. We hypothesized it might be possible to expand progenitor cells—without a priori knowledge of the exact exogenous signaling factors required for their maintenance in vitro—merely by ectopically expressing key genes. We identify six factors, *Gata2*, *Lmo2*, *Mycn*, *Pitx2*, *Sox17*, and *Tal1*, that collectively

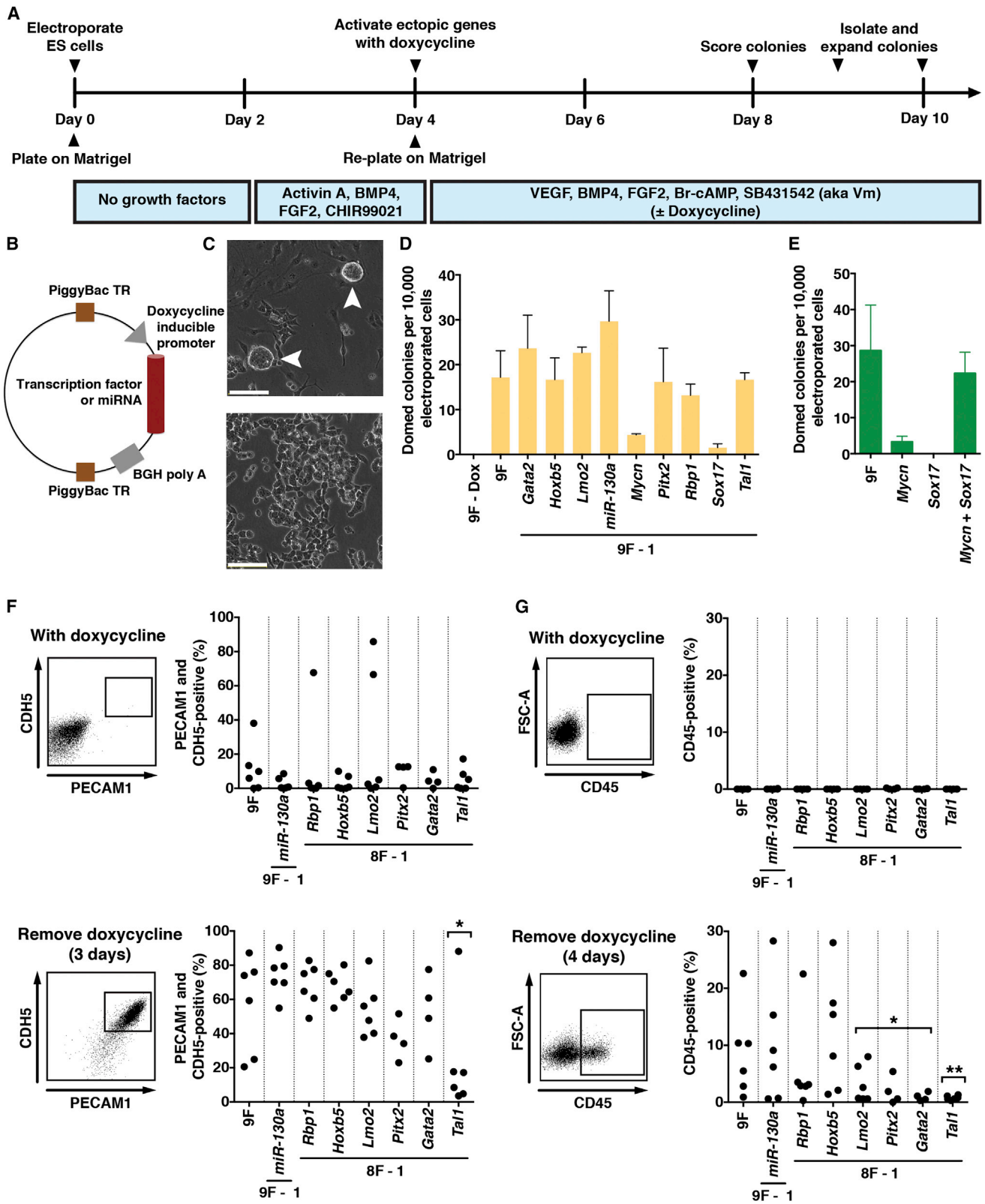

(legend on next page)

establish and maintain a proliferative state with hemangioblast potential.

RESULTS

Identifying Factors that Maintain Hemangioblast Potential

We screened for factors that might maintain hematopoietic progenitors in culture by examining candidate genes that either had literature support for their role in hematopoiesis (for example, Chambers et al., 2007; Elcheva et al., 2014; Petriv et al., 2010) and/or were expressed in FL HSCs. The screen involved electroporating combinations of transcription factors and miRNAs encoded on doxycycline inducible cassettes into murine ESCs stably via the PiggyBac transposase system (Figures 1A and 1B). Electroporated cells were differentiated on Matrigel, following a previous established protocol (Chiang and Wong, 2011), to mesoderm cells, and then doxycycline was added to activate the ectopic genes as the cells were further differentiated toward hemogenic endothelium. Four days after the introduction of doxycycline, rare domed colonies formed with tight, defined edges (Figure 1C, top image). The colonies, composed of small adherent cells, occurred at a frequency of 1 to 2 of 1,000 ESCs transfected with a combination of eight transcription factors and one miRNA, and did not arise in transfected cell populations in the absence of doxycycline (Figure 1D, compare first two bars; data not shown). The domed colonies were observed in multiple independent ESC lines (Figure 1E, first bar). These colonies resembled early blast colonies before they differentiate into both endothelial and hematopoietic cells (Lancrin et al., 2009), except that they continued to grow without apparent differentiation.

In the presence of doxycycline, the cells in the domed colonies were often expandable; that is, the colonies could be picked under a dissecting microscope, gently dissociated with EDTA, and replated on Matrigel and continue to proliferate. The expanding colonies (cultured 11 to 21 days) tended to lose their domed morphology, forming loose associations of scattered cells (Figure 1C, bottom image). When doxycycline was withdrawn from the expanded populations of cells in N2B27 medium supplemented with the growth factors BMP4, FGF2, VEGF, and the small molecules SB431542 and Br-cAMP (vasculogenic mixture or Vm, following the naming convention used previously; Chiang and Wong, 2011), the cells expressed PECAM1 and CDH5, surface markers of endothelial cells, at efficiencies ranging from 21% to 87% (Figure 1F, compare top and bottom graphs, first column). When released from doxycycline and placed in medium supplemented with stem cell factor (SCF), Wnt agonist CHIR99021, interleukin-3, and FLT3L (referred to collectively as SCIF), factors that favor early hematopoiesis (Ruiz-Herguido et al., 2012; Taoudi et al., 2008), in a hypoxic (1.5% O_2) atmosphere, cells were observed to express the canonical hematopoietic marker CD45 (Figure 1G, compare top and bottom graphs, first column). The ability of the isolates to generate $CD45^+$ cells was less efficient and even more variable (1% to 23% of the population) than the ability of the same isolates to produce endothelial-like cells, suggesting that the emergence of the blood cells required a more complex configuration of ectopic factors to be present in the isolates.

To determine which of the nine factors might be responsible for these phenotypes, dropout experiments were conducted. Each of these nine factors was removed one at a time from the combination to determine which were required for domed colony formation. The removal of *Mycn* or *Sox17* reduced colony numbers by 4- or 11-fold, respectively (Figure 1D). Conversely, *Mycn* and *Sox17* together drove the formation of domed colonies in three independent ES lines with frequencies comparable to cells transfected with all nine factors (Figure 1E), although the colony sizes induced by the two factors alone tended to be smaller (data not shown). Next, to determine which factor(s) were required for the production of endothelial or blood cells, additional dropout experiments were

Figure 1. Screening for Hemangioblasts

(A) Overview of the screening procedure.

(B) Schematic representation of the inducible expression vectors employed.

(C) An example of domed colonies arising 4 days after induction with doxycycline (top image). An example of passaged (expanded) colonies 14 days after induction with doxycycline (bottom image). Both images are phase contrast. White bars represent 100 μm.

(D) Average colony number ± SD from at least three independent experiments in one ES line.

(E) Average colony number ± SD in three independent ES lines.

(F and G) Five domed colonies were pooled from each well and expanded in Vm containing doxycycline. The resulting isolates were evaluated by FACS. Example FACS dot plots are presented to the left; the box indicates cells considered positive for the marker(s) in isolates maintained with doxycycline (top graph) or the same isolates devoid of doxycycline for the indicated times (bottom graph). For each combination of factors, the results are independent experiments from two ES lines with at least one isolate per line. (F) Endothelial markers. (G) Hematopoietic marker employing the same isolates from (F) (*$p < 0.05$, **$p < 0.01$, Wilcoxon rank sum test, one sided, comparing results with those from all nine factors).

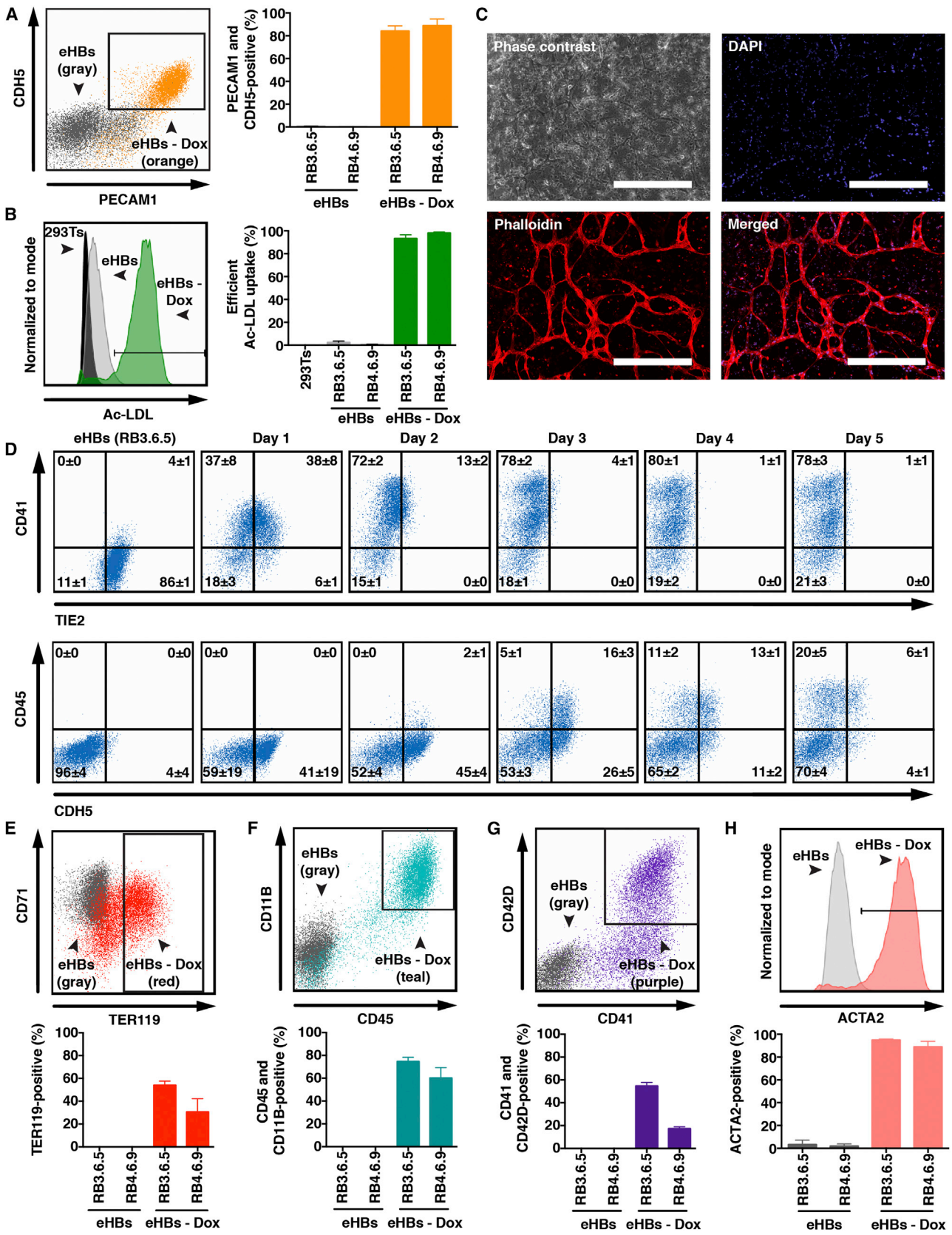

(legend on next page)

performed (Figures 1F and 1G). In these experiments, *Mycn* and *Sox17* were always present in the factor combination to ensure colony formation. The experiments revealed that the absence of *Tal1* significantly reduced the ability of the isolates to express endothelial markers upon the withdrawal of doxycycline (Figure 1F). In addition, the absence of *Lmo2*, *Pitx2*, *Gata2*, or *Tal1* significantly reduced the ability of the isolates to produce CD45$^+$ cells (Figure 1G). These data together indicated that six transcription factors, *Gata2*, *Lmo2*, *Mycn*, *Pitx2*, *Sox17*, and *Tal1*, collectively imposed a program in cells that (1) trapped them in a proliferative state and (2) endowed them with the potential to differentiate toward either blood or endothelial fates, once one or more of the factors was downregulated by the removal of doxycycline.

Expandable Hemangioblasts Give Rise to Functional Endothelial Cells, Multilineage Blood Cells, and Smooth Muscle Cells

Single colonies, now derived with only the six transcription factors in independent ES lines, were isolated, expanded, and cryopreserved. The cells, which we dubbed "expandable hemangioblasts" (eHBs), were confirmed to express all six factors ectopically (Figure S1A available online) and then were tested for their ability to differentiate to select cell types once released from the progenitor state by the withdrawal of doxycycline.

First, cells were cultured in Vm for 3 days. In contrast to control cells maintained with doxycycline, these cells dually expressed the endothelial markers PECAM1 and CDH5 (Figure 2A) and efficiently took up acetylated low-density lipoprotein (Ac-LDL) (Figure 2B). The cells were furthermore able to form capillary-like tubular networks (Figure 2C) with lumen (Figure S1B) when embedded within Matrigel. Collectively, these data indicate that eHBs can differentiate into functional endothelial cells.

The eHBs were next cultured in medium supplemented with SCIF in a hypoxic (1.5% O_2) atmosphere to induce hematopoiesis. We employed markers previously used to trace the ontogeny of hematopoietic populations in early sites of hematopoiesis, including the yolk sac and AGM region (Nishikawa et al., 1998; Taoudi et al., 2008) and/or used to trace the differentiation of hemangioblasts to hematopoietic cells through an endothelial-like state (hemogenic endothelium) (Lancrin et al., 2009). In a time-dependent fashion, the eHBs appeared to give rise to blood progeny by transiting through an intermediate state in which the endothelial markers TIE2 or CDH5 were coexpressed with the blood markers CD41 or CD45 (Figures 2D and S1C). The transient CDH5$^+$ cells were able to take up Ac-LDL (Figure S1D), which supports the notion of their endothelial-like nature, although their ability to do so was not as efficient as the eHB-derived endothelial cells (compare Figures 2B and S1D). To confirm that the blood cells indeed arose from these putative hemogenic endothelial intermediates, the differentiating cells were sorted into CDH5$^+$ and CDH5$^-$ populations 2 days into the culture and then cultured for 2 days further. The CDH5$^+$ cells robustly gave rise to CD45$^+$ cells, in contrast to their CDH5$^-$ counterparts (Figure S1E). These data indicate that eHBs give rise to blood cells through an endothelial-like intermediate state, in a manner consistent with previously described emerging hematopoietic populations either in vitro or in vivo.

The eHBs were next tested for their ability to produce hematopoietic cells of different lineages. When placed in conditions akin to those previously described to promote erythropoiesis (Sturgeon et al., 2012), the cells gave rise to TER119$^+$ erythrocytes (many of which were also CD71$^+$; Figure 2E) that abundantly expressed embryonic hemoglobin, but quite poorly expressed adult hemoglobin (Figure S1F). This result indicates that the eHBs preferentially give rise to primitive hematopoiesis. When differentiated

Figure 2. Characterization of the eHBs

(A and B) Endothelial differentiation (3 days). (A) Endothelial markers. (B) Cells were incubated with fluorescently labeled Ac-LDL for 2 hr; 293T cells were employed as a negative control. The bar identifies cells efficiently taking up Ac-LDL.

(C) Formation of capillary-like networks in Matrigel. Cells were differentiated for 7 days in Vm and then embedded in Matrigel for 10 days. White bars represent 400 μm.

(D) Hematopoietic differentiation time course. The values represent the average percent of cells in each quadrant ± SD measured by FACS in three independent experiments of the eHB line RB3.6.5.

(E) Erythrocyte differentiation (4 days).

(F) Macrophage differentiation (9 days).

(G) Megakaryocytes/proplatelet differentiation (4 days).

(H) Smooth muscle differentiation (3 days).

All example dot plots, images, and histograms are from the eHB line RB3.6.5. Two independent eHB cell lines (each established from a single colony) were maintained with doxycycline in Vm or differentiated in the absence of doxycycline ("−Dox"). (A and E–G) Example FACS dot plots are provided for each assay. The box indicates cells considered positive for the markers; these values are summarized in the adjacent bar graphs as the average percent of positive cells ± SD from three independent experiments of each line. (B and H) Example histograms are provided for each assay. The bar represents cells considered positive. These values are compiled in the adjacent bar graphs as the average percent of cells ± SD from at least three independent experiments of each line. See also Figure S1 and Table S1.

in conditions similar to those previously employed to generate macrophages (Choi et al., 2011), the eHBs produced $CD45^+/CD11B^+$ (Mac-1) macrophages (Figures 2F and S1G). When differentiated in Stemline II medium (Sigma) supplemented with SCIF and the megakaryocyte cytokine TPO, the cells gave rise to megakaryocytes and proplatelets, as indicated by the dual expression of the markers CD42D (Takada et al., 1995) and CD41 (Figure 2G) and the presence of multinucleated cells (Figure S1H). Finally, when differentiated in medium supplemented with SCIF, the eHBs also produced, albeit quite inefficiently, BFU-Es (erythrocyte progenitors), CFU-G/M/GMs (granulocyte and/or macrophage progenitors), and CFU-GEMMs (granulocyte, erythrocyte, macrophage, and megakaryocyte progenitors) (Figure S1I). Together, these data indicate the eHBs, when released from control of the ectopic factors, are capable of undergoing multilineage hematopoiesis.

Next, the eHBs were assayed for their potential to give rise to smooth muscle cells, a capacity also attributed to hemangioblasts (Yamashita et al., 2000). After 3 days, differentiation on collagen IV in conditions previously shown to promote the differentiation of smooth muscle cells (Xiao et al., 2007), the eHBs gave rise to progeny (Figure S1J) that expressed smooth muscle actin (ACTA2) and the additional smooth muscle markers *Cnn1* (calponin 1), *Myh11* (*smMHC*), and *Tagln* (*Sm22α*) (reviewed in Owens, 1995) (Figures 2H and S1K). These data indicate that besides blood and endothelial potential, the eHBs also possess smooth muscle potential.

Finally, we challenged the eHBs to give rise to cells not considered to be the progeny of hemangioblasts. The cells were tested for their ability to produce cardiomyocytes, which arise from progenitors that are related to hemangioblasts, but distinguishable from them (Kattman et al., 2006, 2011). Aggregates of eHBs and their parent ESC lines were differentiated in conditions based on previous studies (Sargent et al., 2009; Zhang et al., 2012) designed to promote cardiomyocyte differentiation. In contrast to the ESC lines, spontaneously beating cardiomyocytes did not arise detectibly from the eHBs (Figures S1L and S1M). Instead, at least some of their surviving progeny appear to differentiate into smooth muscle cells under these conditions (Figure S1M). Taken together, these data suggest that when released from the ectopic factors, the eHBs preferentially give rise to blood and vascular lineages, evidence that supports their putative hemangioblast identity.

To determine how long in culture the six ectopic factors could maintain the eHB state, two eHB lines were passaged heavily—approximately 117 population doublings, an expansion of over 10^{35} from the founding cells—and then differentiated into endothelial, blood, or smooth muscle cells (Figure S1N). Even after this extensive passaging, both cell lines were still competent to produce the three cell types, but tended to do so with a reduced efficiency, an effect associated in one line with the silencing of ectopic *Gata2* (Figure S1A).

The Six Factors Can Induce the eHB State

As described above, the same set of factors that maintain the ES pluripotent state in culture also can induce this state in somatic cells. Although we had originally identified the six transcription factors as those that could maintain a hemangioblast state, we supposed that these factors might also induce the state. To test this notion, we transfected mouse embryonic fibroblasts (MEFs) or embryonic day 14.5 FL cells with the six factors and cultured them in the presence of doxycycline. The MEFs were employed as a test of transdifferentiation and the FL cells as a test of either transdifferentiation or dedifferentiation because the FL, at this stage, is a hematopoietic organ. Approximately 1 week after transfection, colonies with eHB morphology emerged from either source, at an observed frequency of almost 1:1000 transfected cells (Figures 3A and 3B). Three independent eHB lines expressing the six factors ectopically (Figure S2A) derived from MEF or FL cells were established from single colonies and assayed for their ability to give rise to endothelial (Figures 3C, 3D, S2B, and S2C), blood (Figures 3E, 3F, S2D, and S2E), and smooth muscle (Figures 3G and S2F) cells in the absence of doxycycline. The FL-eHBs were able to produce all three cell types. However, the MEF-eHBs tended to perform more poorly, particularly in the production of blood or smooth muscle cells, indicating that the factors do not fully reprogram MEFs, at least in the lines examined.

The eHBs derived from cultured cells (ESCs or MEFs) were often found with missegregations of the Y chromosome, possessing XYY, XO, or both (Table S1). This result parallels the previously known instability of the Y chromosome in cultured murine ESCs (Eggan et al., 2002), except that here we detect cells not only containing XO, but also the counterpart XYY. However, all eHBs derived from uncultured FL cells tested so far possess a normal karyotype. These data indicate that primary cells (or perhaps female cells) may be the best sources from which to derive the eHBs.

RNA-Seq Analysis of eHBs and Their Derivatives

The eHBs were next analyzed globally by RNA-seq to further assess their developmental status. We examined the transcriptomes of lines derived from ESC, FL, or MEF sources as well as their differentiated progeny and compared them with those of ESCs, ESC-derived KDR^+ mesoderm cells (a population of cells that includes early hemangioblasts), and primary cell populations enriched for either embryonic endothelial cells (embryonic day 11.5 $PECAM1^+/CDH5^+$ cells dissociated from either the yolk sac or embryo), or FL HSCs (embryonic day 14.5

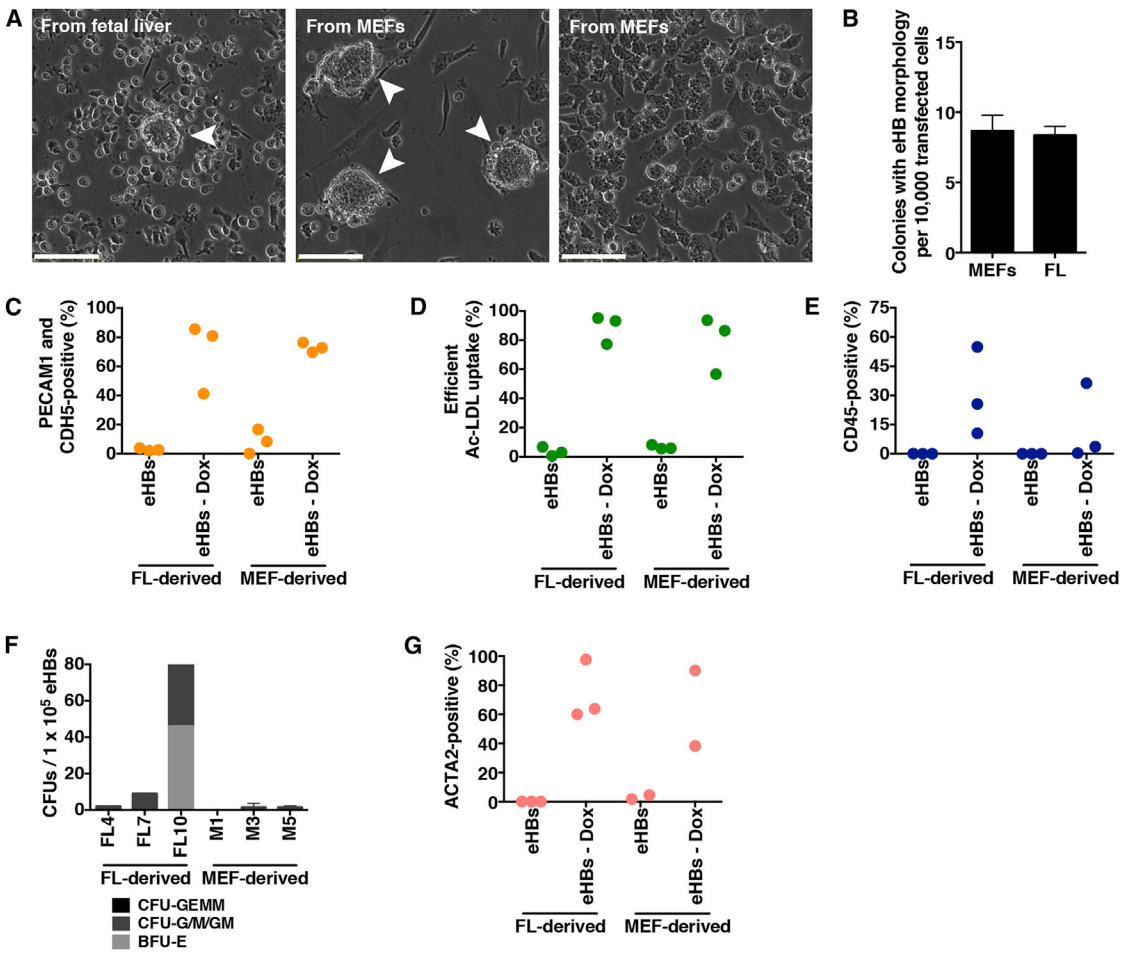

Figure 3. The eHBs Can Be Derived from Different Cell Sources

(A and B) Colonies present 8 days (E14.5 FL cells) or 7 days (MEFs) after transfection. (A) Example phase contrast images of colonies. The eHBs can arise as domed colonies (left and middle images) and/or scattered colonies (right image). White bars represent 100 μm. (B) Quantification of domed and/or scattered eHB colonies. Results are the average ± SD of three independent experiments.

(C–E and G) FACS analysis of endothelial (C and D), blood (E), and smooth muscle (G) cells arising from the eHBs, differentiated as described in Figures 1 and 2. The results from three independent lines, each established from a single colony derived from FL or MEF cells, are shown for every assay (each line tested once), except for (G), which shows results from only two MEF-eHB lines because the third repeatedly failed to produce sufficient live differentiated cells for analysis.

(F) Hematopoietic CFUs from the indicated eHB lines. Results are from one (FL lines) or two (MEF lines, average ± SD shown) independent experiments.

The eHB lines were induced and maintained with doxycycline in N2B27 medium supplemented with FGF2. See also Figure S2 for additional data including example FACS dot plots, histograms, and images of hematopoietic colonies and Table S1.

$CD150^+/CD201^+/CD48^-/CD45^+$ cells). We chose this latter cell type for comparison because it is a well-defined population of early hematopoietic progenitors (Kent et al., 2009). The KDR^+ mesoderm cells were obtained by differentiating ESCs 4 days as described in Figure 1A. The eHB-derived cells analyzed included the hematopoietic populations $CDH5^+/CD45^-$ and $CDH5^+/CD45^+$ (differentiated 2 or 3 days, respectively, as described in Figure 2D) and endothelial cells (differentiated 3 days as described in Figure 2A). When the transcriptomes of these populations were compared by principal component analysis (Figure 4A) or unsupervised hierarchical clustering (Figure 4B), a clear tendency was revealed. The eHBs grouped near ESC-derived KDR^+ mesoderm cells and away from ESCs. The endothelial progeny of the eHBs grouped with the primary endothelial cells; the blood progeny of the eHBs grouped with FL HSCs. These data suggested the eHBs are trapped at or downstream of mesoderm development.

The examination of key marker genes further pinpointed the developmental state of the eHBs. In agreement with

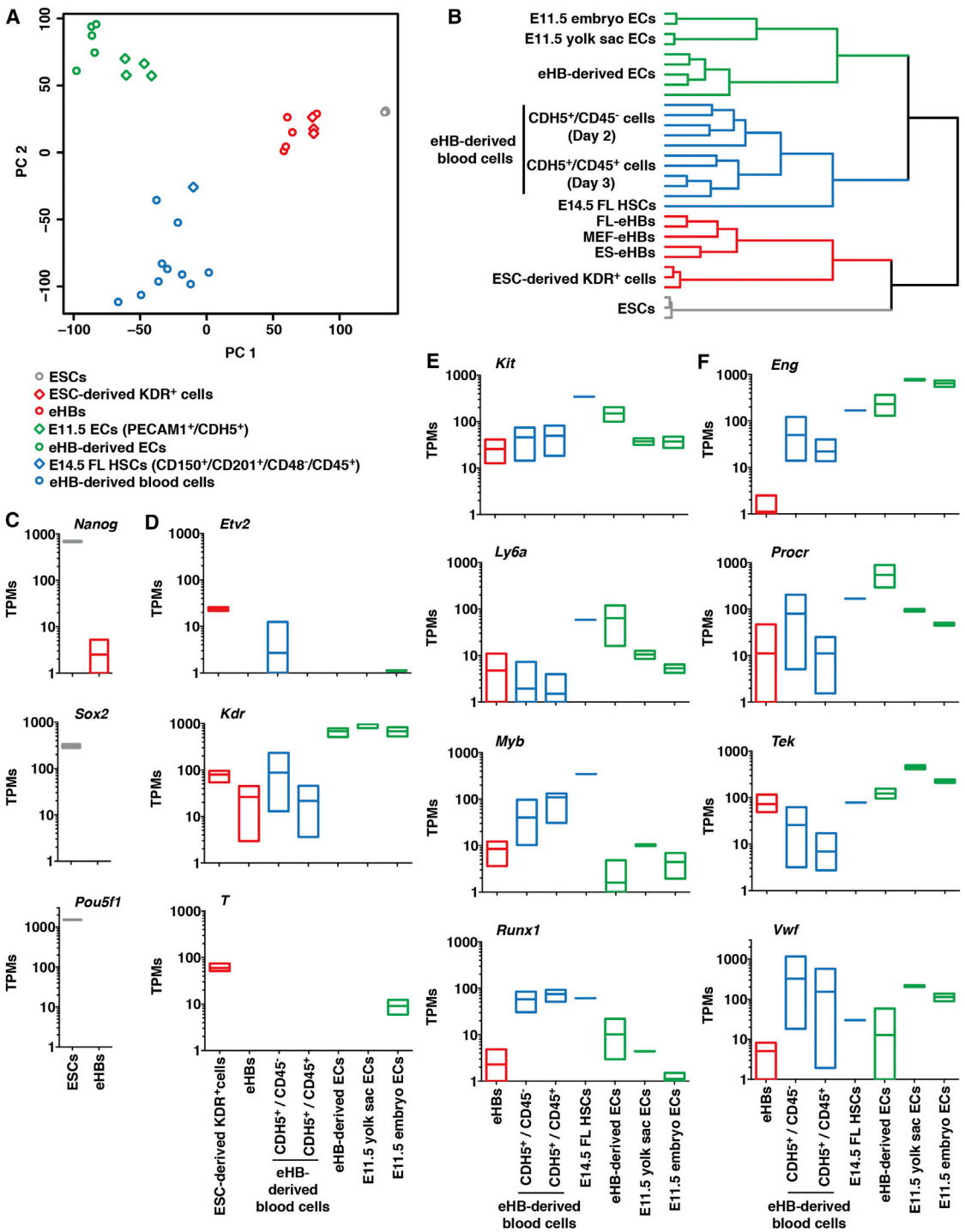

Figure 4. RNA-Seq Uncovers the Developmental State of the eHBs

(A) Principal component analysis.

(B) Unsupervised hierarchical clustering.

(C–F) Expression levels of select marker genes measured by RNA-seq. The y axes are in $\log_{10}$ scaling with a threshold of detection cutoff of 1 transcript per million (TPM). Box sizes represent the minimum to maximum TPM values of the samples described in (A) and (B); the line inside the boxes represents the mean. (C) ESC markers. (D) Mesoderm markers. (E) Hematopoietic markers. (F) Endothelial markers.

RNA-seq analysis was performed on ESCs and their derivatives, on eHBs and their derivatives, on primary E14.5 FL HSCs, and on primary E11.5 endothelial cells (ECs). Five eHB lines were employed, two derived from ESCs, two derived from FL cells, and one derived from MEFs. See also Figure S3 and Table S1.

the clustering, canonical ESC genes like *Pou5f1* (*Oct4*) and *Sox2* are not expressed in the eHBs, and *Nanog* is poorly detected (Figure 4C). The eHBs express a number of genes associated with mesoderm (Figure S3A), but do not express the transiently expressed mesoderm regulator *T* (*Brachyury*) or *Etv2* (*Er71*) (Figure 4D), a mesoderm factor expressed concomitantly with *T* that is required for the formation of the endothelial and hematopoietic lineages, in part by upregulating *Kdr* (*Flk1*) (Lee et al., 2008). *Kdr* is inefficiently expressed in eHBs (Figure 4D), and the several lines tested by fluorescence-activated cell sorting (FACS) do not robustly stain for this marker (data not shown). The downregulation of *Kdr* is likely due to the ectopic expression of *Sox17*, as has been previously observed (Nakajima-Takagi et al., 2013). This notion is supported by the observation that *Kdr* expression increases in the endothelial or hemogenic endothelial ($CDH5^+/CD45^-$) progeny of the eHBs, as the ectopic expression of *Sox17* diminishes (Figures 4D and S3B). These data indicate that eHBs are developmentally trapped downstream of *T* and *Etv2* expression and thus do not resemble early, canonical blast colony-forming cells (BL-CFCs) (Choi et al., 1998; Faloon et al., 2000; Fehling et al., 2003; Huber et al., 2004).

The blood or endothelial derivatives of eHBs express a number of hematopoietic and endothelial markers (Figures 4E, 4F, S3B, and S3C). However, while the emerging blood cells generated from the eHBs express *Erg*, they fail to express *Hoxa9* and *Rora* (Figure S3C). Collectively, these three factors have been previously shown to expand human blood progenitors with high CFU potential (Doulatov et al., 2013). The absence of *Hoxa9* and *Rora* provides a possible explanation for why the eHBs generate CFUs poorly (Figures 3F and S1I). The blood derivatives of the eHBs poorly express the definitive hematopoietic progenitor markers *Kit*, *Ly6a* (*Sca1*), or *Procr* (*Epcr*) (Figures 4E and 4F), an additional indication that the eHBs preferentially give rise to primitive hematopoiesis. The endothelial progeny of the eHBs better express these three markers, suggesting they may possess hemogenic potential, although this has not been observed. The endothelial progeny of the eHBs do not efficiently express the endothelial marker *VWF* (Figure 4F); however, this marker has variable expression across the developing murine vasculature (Coffin et al., 1991). The $CDH5^+/CD45^-$ progeny of the eHBs upregulate a number of endothelial genes whose expression then tends to diminish as the cells acquire CD45 expression (Figures 4D and 4F), further supporting the transiently endothelial-like nature of these cells.

A Central Role for FGF

Because eHBs are trapped in a progenitor state, they afford the unique opportunity to examine growth factor signaling on a hemangioblast state prior to its commitment to a particular fate. The ESC-derived eHBs were originally found and maintained with doxycycline in Vm (N2B27 medium supplemented with the growth factors BMP4, FGF2, VEGF, and the small molecules SB431542 and Br-cAMP). In these conditions, the cells associate loosely, migrate as single cells or small groups ("scatter"), and at higher densities form flatter colonies with occasional domed colonies (Figure 5A; Movie S1). The morphology of the cells changes as they move: the cells elongate, contract, and often exhibit pronounced lamellipodia. In Vm with doxycycline, the cell populations double on average every 16 hr (Figure 5B). In N2B27 medium containing doxycycline without any additional growth factors, the doubling slowed to an average of every 37 hr, and the cells converted to growth in domed colonies, reminiscent of how they often emerge prior to passaging ("No GFs" Figures 5A and 5B; Movie S2). These observations indicated that one or more of the exogenous factors present in Vm were responsible for stimulating the eHBs to change their growth and morphological characteristics. To determine which factor(s) might be responsible, eHBs were maintained with doxycycline in N2B27 medium supplemented with single additional growth factors. In contrast to the addition of BMP4, the addition of FGF2 alone was sufficient to cause the cells to expand more efficiently, to scatter, and to form flatter colonies (Figures 5A and 5B; Movie S3). The ability of FGF2 to exert these effects was not appreciably altered by the additional presence of BMP4 (Figures 5A and 5B).

To determine the means by which FGF2 was altering the growth and morphological characteristics of the eHBs, small molecule inhibitors were employed. For these assays, each inhibitor was titrated on the cells growing in N2B27 medium containing doxycycline and FGF2. In a dose-dependent manner, PD173074, a high-affinity inhibitor of the FGF receptor, phenocopied the absence of FGF2 (Figures 5C and 5D), indicating that FGF2 signals through its canonical receptors. The FGF receptors target multiple signaling pathways, including the MAPK/ERK or PI3K pathways (reviewed in Eswarakumar et al., 2005). Indeed, the MEK (ERK kinase) inhibitors PD0325901 and U0126, or the PI3K inhibitor PI828, all revealed a dose-dependent inhibition on the expansion of the eHBs (Figure 5C). However, each of these three inhibitors alone could not fully mimic the morphological changes that occur in the absence of FGF2 (Figure 5D). Instead, the dual inhibition of the MEK and PI3K pathways better imitated the loss of FGF2 (less so with U0126, markedly with the higher affinity MEK inhibitor PD0325901) in the eHB line RB3.6.5. Furthermore, the PI3K activator 740 Y-P alone failed to promote the expansion of the eHBs in the absence of FGF2 (Figure 5E), supporting the notion that FGF2 exerts its effects on the eHBs through both MEK and PI3K signaling. It is not yet clear whether FGF2 activates additional

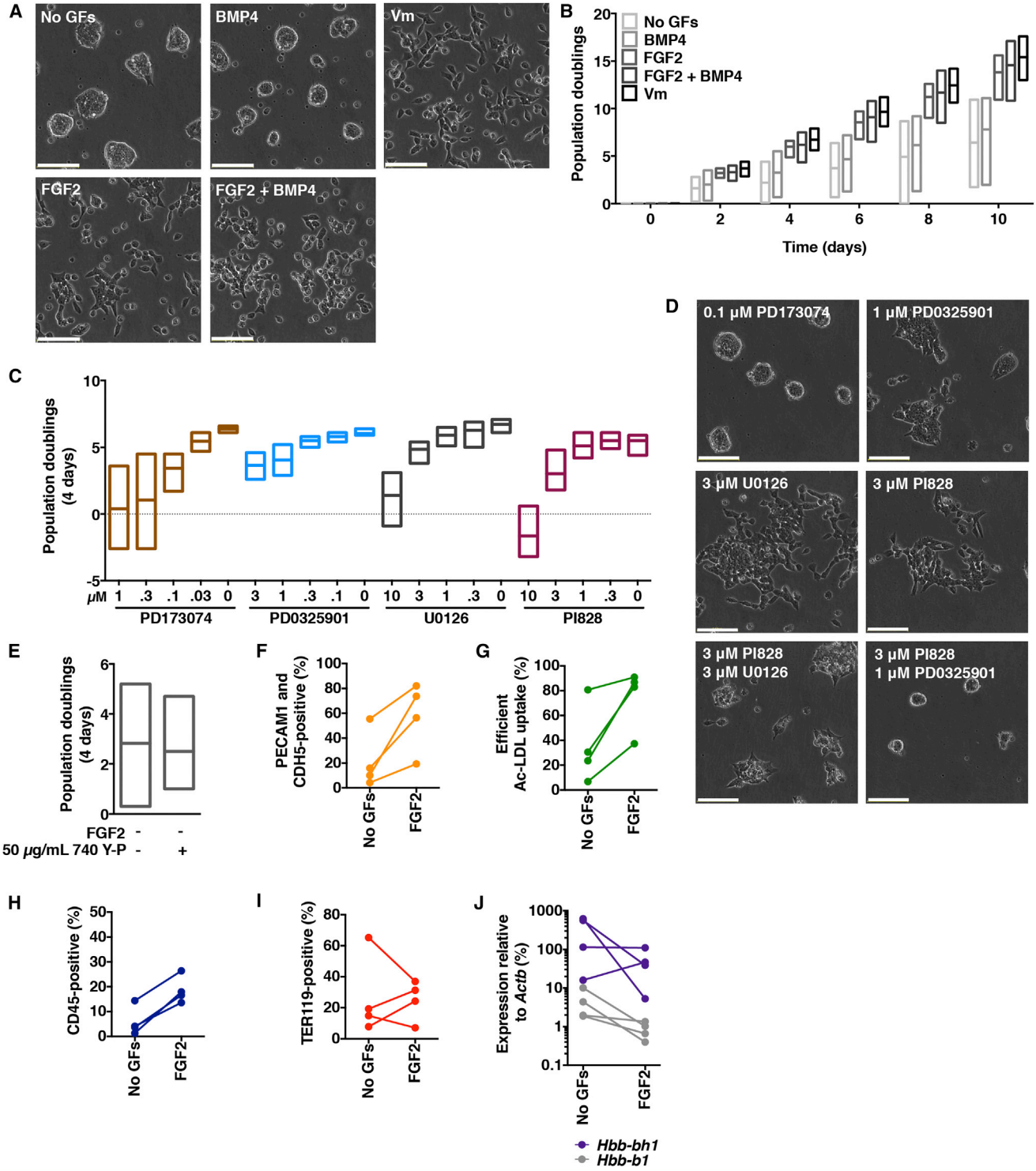

Figure 5. The Effect of FGF on the eHBs

(A) Phase contrast example images of the eHB line RB3.6.5 in different maintenance media. White bars represent 100 μm.

(B) Growth curve of eHB lines in different maintenance media.

(C) Titration of small molecule inhibitors in N2B27 medium containing doxycycline and FGF2.

(D) Phase contrast example images of the eHB line RB3.6.5 grown in medium as (C) for 2 days in the presence of the indicated small molecule inhibitors. White bars represent 100 μm.

(legend continued on next page)

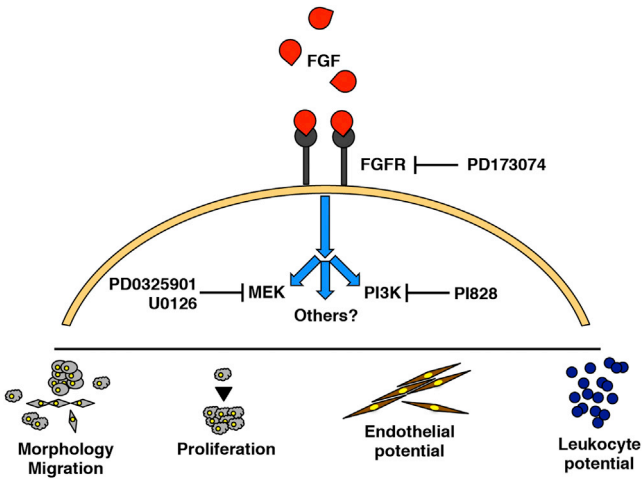

Figure 6. Proposed Model for the Role of FGF in the eHBs
The binding of FGF to its receptor(s) (Plotnikov et al., 1999) appears to foster signaling in the eHBs through at least the MEK and PI3K signaling pathways. Perhaps collectively, these pathways (1) alter the morphology and migration of the eHBs, (2) cause the eHBs to expand efficiently, and (3) prime the eHBs to generate endothelial cells and leukocytes. The small molecule inhibitors employed in this study and their targets are depicted.

signaling pathways in the eHBs, for example, the protein kinase C pathway (Eswarakumar et al., 2005).

We wondered if, besides altering the proliferation and morphology of the eHBs, FGF2 might also be altering their fate decisions. Therefore, four independent eHB cell lines were tested for their ability to produce endothelial cells (Figures 5F and 5G), leukocytes (scored broadly as $CD45^+$ cells; Figure 5H), and erythrocytes (Figures 5I and 5J) after being maintained in the absence or presence of FGF2. Cells maintained only in N2B27 medium with doxycycline tended to produce endothelial cells or leukocytes poorly. In contrast, cells additionally supplemented with FGF2 were better able to generate these cell types. This trend did not hold for the production of erythrocytes (Figures 5I and 5J). FGF2 did not consistently improve the efficiency by which the eHBs produced these cells; in fact, in some lines, the absence of FGF correlated with improved erythropoiesis (and improved viability of the differentiated cells, data not shown), a finding consistent with previous observations (Weng and Sheng, 2014). Taken together, these data indicate that FGF2 signaling is a key influence on the eHBs, promoting their expansion, altering their morphology, and poising them for vasculogenesis and leukopoiesis but not erythropoiesis.

DISCUSSION

We have uncovered a set of six transcription factors, *Gata2*, *Lmo2*, *Mycn*, *Pitx2*, *Sox17*, and *Tal1*, that collectively maintain cells in culture with the ability to give rise to blood, endothelial, or smooth muscle progeny. In the continued presence of the transcription factor(s), the progenitor populations expand over many generations and commit to a differentiation program as the ectopic factor(s) are downregulated by the withdrawal of doxycycline. We hypothesize the ability of the eHBs to remain in a proliferative progenitor state is a result of the enduring expression of *Mycn* and *Sox17* because these two factors are central for colony formation. The loss of *Sox17* disrupts hematopoiesis in the yolk sac and, more profoundly, within the embryo (Kim et al., 2007). Recently, the transient, enforced expression of *Sox17* has been found to expand a hemogenic endothelial population that gives rise to multilineage hematopoietic cells (Clarke et al., 2013; Nakajima-Takagi et al., 2013). This activity is thought to occur through the Notch signaling pathway. Notch signaling also regulates *Myc* in murine hematopoietic progenitors (Satoh et al., 2004), but to our knowledge, it is unknown whether it likewise regulates *Mycn*. However, given the parallel functions of *Myc* and *Mycn* (Malynn et al., 2000), these data suggest the hemangioblast state might in part be maintained by persistent Notch signaling. Both *Mycn* and *Sox17* are employed repeatedly during development, and it is thus no surprise that they apparently are not enough, on their own, to maintain a hemangioblast state. This task, we hypothesize, is aided by the other four factors. Indeed, *Gata2*, *Lmo2*, or *Tal1* null embryos all die early in development with extreme hematopoietic deficiencies

(E) Growth in N2B27 medium containing doxycycline, with or without the PI3K activator 740 Y-P (Tocris).
(F–I) FACS analysis of the differentiated progeny from four independent eHB lines (each line tested at least once, for replicates the average is shown) maintained in N2B27 medium containing doxycycline, with or without FGF2. Differentiated and scored as exemplified in Figures 1 or 2. (F and G) Endothelial differentiation. (F) Endothelial markers. (G) Ac-LDL uptake. (H) The pan-leukocyte marker CD45. (I) The erythrocyte marker TER119.
(J) Measurements by quantitative PCR of the expression level of embryonic (*Hbb-bh1*) and adult hemoglobin (*Hbb-b1*) in cultures described in (I). The y axis is on a $\log_{10}$ scale.
Results are from eHB cell lines maintained with doxycycline in N2B27 medium ("No GFs") or in N2B27 medium supplemented with FGF2, BMP4, both FGF2 and BMP4, or Vm. (B, C, and E) Box sizes represent the minimum to maximum number of cumulative population doublings measured at the indicated times in four to five independent eHB lines (each tested at least once); the line inside the boxes represents the mean. Two ESC-derived eHBs and two or three FL-derived eHBs were employed. See also Table S1 and Movies S1, S2, and S3.

(Shivdasani et al., 1995; Tsai et al., 1994; Warren et al., 1994). Ectopic *Lmo2*, in concert with *Mycn*, *Hlf*, *Meis1*, *Pbx1*, *Prdm5*, *Runx1t1*, and *Zfp37*, has recently been shown to reprogram blood cells to definitive HSCs (Riddell et al., 2014). Ectopic *Gata2*, *Tal1*, and *Etv2* promote the development of murine hemangioblasts, although it is not clear whether this combination of factors can sustain the expansion of the cells, or induce them from sources other than ESCs (Liu et al., 2013).The expression of *Pitx2* is specific to HSCs when compared with differentiated blood cells (Degar et al., 2001), and *Pitx2* null embryos die early with a number of developmental defects (Lin et al., 1999; Lu et al., 1999). However, *Pitx2* null HSCs do arise and give rise to differentiated blood progeny (Zhang et al., 2006), likely indicating some functional redundancy for this factor's participation in hematopoiesis in vivo.

We exploited the fact that the eHBs were trapped as progenitors to analyze the effect of specific growth factors upon them and uncovered a central role for FGF (Figure 6). These data are consistent with studies in which FGF promoted the expansion of BL-CFCs derived from human or murine ESCs (Faloon et al., 2000; Vodyanik et al., 2010) and high proliferative potential hemangioblasts from the murine AGM (Yao et al., 2007). The eHBs provide a tractable means to study in fine detail the function of FGF or any other growth factors on the development of the blood and blood vessel lineages.

Our study parallels the work of other groups who have demonstrated the capacity of ectopic factors to expand progenitors in vitro; for example, *HOXB4* or *Myc* have been used to briefly propagate murine hematopoietic progenitors (Satoh et al., 2004; Sauvageau et al., 1995). More recent examples include employing *BCL-XL*, *BMI1*, and *MYC* to expand human megakaryocyte progenitors (Nakamura et al., 2014); *Myc*, *Sox2*, and an shRNA targeting p53 to expand human erythroid progenitors (Huang et al., 2014); and *ERG*, *HOXA9*, *MYB*, *RORA*, and *SOX4* to expand human hematopoietic progenitors with multilineage potential that can transiently give rise to erythroid or myeloid cells in vivo (Doulatov et al., 2013). The ability to efficiently expand progenitors has broad implications; by identifying the "resident" proto-oncogenes in a given progenitor cell and then controlling them ectopically, it may be possible to trap, expand, and study many other types of progenitor cells and their differentiated progeny, particularly those that are not currently able to be maintained in culture.

EXPERIMENTAL PROCEDURES

Mice Strains

The following strains of mice were employed: B6.SJL-*Ptprc*^{a} *Pepc*^{b}/BoyJ (Jackson, stock number 002014) and B6.Cg-*Gt(ROSA)26Sor*$^{tm1(rtTA*M2)Jae}$/J (Jackson, stock number 006965). Animal experiments and procedures were approved by the University of Wisconsin-Madison School of Medicine and Public Health Animal Care and Use Committee and were conducted in accordance with the Animal Welfare Act and Health Research Extension Act.

DNA Vectors

The cDNAs for rat *Gata2* and murine *Lmo2*, *Tal1*, *Sox17*, *Mycn*, *Pitx2*, *Hoxb5*, and *Rbp1* were obtained from Open Biosystems or GeneCopoeia encoded on Gateway Entry vectors or subsequently cloned into them. The sequence encoding *miR-130a* was amplified by PCR from murine genomic DNA and cloned into a Gateway Entry vector. All cDNAs on Entry vectors were then cloned, using Gateway LR clonase (Life Technologies), into a doxycycline-inducible expression cassette akin to a previously reported construction (Agha-Mohammadi et al., 2004) flanked by PiggyBac terminal repeats on a Gateway Destination vector. All vectors and their sequences are available upon request.

Isolation, Culture, and Cryopreservation of eHBs

Colonies were picked under a dissecting microscope 5 to 8 days (depending on the starting cell type) after induction with 2 μg/ml doxycycline and dissociated by incubation in HEH (0.5 mM EDTA [Fisher] in 1 × Hank's balanced salt solution supplemented with 10 mM HEPES [both from Life Technologies]) for 5 to 10 min followed by trituration. Cells were pelleted and plated on Matrigel-coated plasticware in medium containing doxycycline. For each passage, typically every 2 days, cells were dissociated with HEH and replated, unless otherwise noted. Karyotype analyses were conducted at the WiCell Research Institute. To efficiently cryopreserve the eHBs, cells were resuspended in N2B27 medium and aliquoted to cyrotubes containing an equal volume of N2B27 medium with 10% DMSO (Sigma), for a final concentration of 5% DMSO, and gently inverted repeatedly to mix. The tubes were frozen in Nalgene "Mr. Frosty" freezing containers at −80°C and then placed in liquid nitrogen. Upon thawing rapidly in a 37°C water bath, cells were removed from tubes using large orifice tips, diluted into N2B27 medium, and pelleted to remove DMSO. All cell lines were cultured at 37°C and 5% CO_2 in humidified incubators.

ACCESSION NUMBERS

The GEO accession number for the RNA-seq data reported in this paper is GSE60896.

SUPPLEMENTAL INFORMATION

Supplemental Information includes Supplemental Experimental Procedures, three figures, one table, and three movies and can be found with this article online at http://dx.doi.org/10.1016/j.stemcr.2014.10.003.

AUTHOR CONTRIBUTIONS

D.T.V. designed and conducted experiments, analyzed data, and wrote the manuscript. V.V. performed experiments described in Figures 2C and S1B. S.A.S. analyzed RNA-seq data for Figures 4 and S3. L.-F.C. guided D.T.V. in the derivation of the murine ESC

lines and analyzed some of the preliminary screening data. B.E.M. commenced the breedings to establish the RosaBoy mouse strain, provided pilot RNA-seq data of FL HSCs, and created the PiggyBac Gateway Destination vector employed here. V.V. and S.A.S. contributed to the writing of the portions of the manuscript with which they were associated. J.A.T. designed and supervised experiments and wrote the manuscript.

ACKNOWLEDGMENTS

This work was supported by the Charlotte Geyer Foundation, the Morgridge Institute for Research, NIH grant 1U01 HL099773-01 (to J.A.T.), and NHGRI training grant (5T32HG002760) to the Genomic Sciences Training Program at the UW (to D.T.V.). J.A.T. is a founder, stock owner, consultant, and board member of Cellular Dynamics International (CDI). We thank Dr. Jihye Yun for her assistance isolating FL HSCs for preliminary RNA-seq and cloning some of the expression vectors. We thank Mitch Probasco and Nick Propson for their assistance sorting cells by flow cytometry; Jen Bolin, Angela Elwell, and Bao Kim Nguyen for the preparation and sequencing of the RNA-seq samples; and Bret Duffin for the animal husbandry. We thank Dr. Bill Sugden and Dr. Igor Slukvin for their critical reading of early drafts of the manuscript.

Received: April 22, 2014
Revised: October 13, 2014
Accepted: October 14, 2014
Published: November 13, 2014

REFERENCES

Agha-Mohammadi, S., O'Malley, M., Etemad, A., Wang, Z., Xiao, X., and Lotze, M.T. (2004). Second-generation tetracycline-regulatable promoter: repositioned tet operator elements optimize transactivator synergy while shorter minimal promoter offers tight basal leakiness. J. Gene Med. *6*, 817–828.

Bendall, S.C., Stewart, M.H., Menendez, P., George, D., Vijayaragavan, K., Werbowetski-Ogilvie, T., Ramos-Mejia, V., Rouleau, A., Yang, J., Bossé, M., et al. (2007). IGF and FGF cooperatively establish the regulatory stem cell niche of pluripotent human cells in vitro. Nature *448*, 1015–1021.

Chambers, S.M., Boles, N.C., Lin, K.Y., Tierney, M.P., Bowman, T.V., Bradfute, S.B., Chen, A.J., Merchant, A.A., Sirin, O., Weksberg, D.C., et al. (2007). Hematopoietic fingerprints: an expression database of stem cells and their progeny. Cell Stem Cell *1*, 578–591.

Chen, G., Gulbranson, D.R., Hou, Z., Bolin, J.M., Ruotti, V., Probasco, M.D., Smuga-Otto, K., Howden, S.E., Diol, N.R., Propson, N.E., et al. (2011). Chemically defined conditions for human iPSC derivation and culture. Nat. Methods *8*, 424–429.

Chiang, P.M., and Wong, P.C. (2011). Differentiation of an embryonic stem cell to hemogenic endothelium by defined factors: essential role of bone morphogenetic protein 4. Development *138*, 2833–2843.

Choi, K., Kennedy, M., Kazarov, A., Papadimitriou, J.C., and Keller, G. (1998). A common precursor for hematopoietic and endothelial cells. Development *125*, 725–732.

Choi, K.D., Vodyanik, M., and Slukvin, I.I. (2011). Hematopoietic differentiation and production of mature myeloid cells from human pluripotent stem cells. Nat. Protoc. *6*, 296–313.

Clarke, R.L., Yzaguirre, A.D., Yashiro-Ohtani, Y., Bondue, A., Blanpain, C., Pear, W.S., Speck, N.A., and Keller, G. (2013). The expression of Sox17 identifies and regulates haemogenic endothelium. Nat. Cell Biol. *15*, 502–510.

Coffin, J.D., Harrison, J., Schwartz, S., and Heimark, R. (1991). Angioblast differentiation and morphogenesis of the vascular endothelium in the mouse embryo. Dev. Biol. *148*, 51–62.

Degar, B.A., Baskaran, N., Hulspas, R., Quesenberry, P.J., Weissman, S.M., and Forget, B.G. (2001). The homeodomain gene Pitx2 is expressed in primitive hematopoietic stem/progenitor cells but not in their differentiated progeny. Exp. Hematol. *29*, 894–902.

Doulatov, S., Vo, L.T., Chou, S.S., Kim, P.G., Arora, N., Li, H., Hadland, B.K., Bernstein, I.D., Collins, J.J., Zon, L.I., and Daley, G.Q. (2013). Induction of multipotential hematopoietic progenitors from human pluripotent stem cells via respecification of lineage-restricted precursors. Cell Stem Cell *13*, 459–470.

Eggan, K., Rode, A., Jentsch, I., Samuel, C., Hennek, T., Tintrup, H., Zevnik, B., Erwin, J., Loring, J., Jackson-Grusby, L., et al. (2002). Male and female mice derived from the same embryonic stem cell clone by tetraploid embryo complementation. Nat. Biotechnol. *20*, 455–459.

Elcheva, I., Brok-Volchanskaya, V., Kumar, A., Liu, P., Lee, J.H., Tong, L., Vodyanik, M., Swanson, S., Stewart, R., Kyba, M., et al. (2014). Direct induction of haematoendothelial programs in human pluripotent stem cells by transcriptional regulators. Nat. Commun. *5*, 4372.

Eswarakumar, V.P., Lax, I., and Schlessinger, J. (2005). Cellular signaling by fibroblast growth factor receptors. Cytokine Growth Factor Rev. *16*, 139–149.

Faloon, P., Arentson, E., Kazarov, A., Deng, C.X., Porcher, C., Orkin, S., and Choi, K. (2000). Basic fibroblast growth factor positively regulates hematopoietic development. Development *127*, 1931–1941.

Fehling, H.J., Lacaud, G., Kubo, A., Kennedy, M., Robertson, S., Keller, G., and Kouskoff, V. (2003). Tracking mesoderm induction and its specification to the hemangioblast during embryonic stem cell differentiation. Development *130*, 4217–4227.

Godin, I.E., Garcia-Porrero, J.A., Coutinho, A., Dieterlen-Lièvre, F., and Marcos, M.A. (1993). Para-aortic splanchnopleura from early mouse embryos contains B1a cell progenitors. Nature *364*, 67–70.

Huang, X., Shah, S., Wang, J., Ye, Z., Dowey, S.N., Tsang, K.M., Mendelsohn, L.G., Kato, G.J., Kickler, T.S., and Cheng, L. (2014). Extensive ex vivo expansion of functional human erythroid precursors established from umbilical cord blood cells by defined factors. Mol. Ther. *22*, 451–463.

Huber, T.L., Kouskoff, V., Fehling, H.J., Palis, J., and Keller, G. (2004). Haemangioblast commitment is initiated in the primitive streak of the mouse embryo. Nature *432*, 625–630.

Ieda, M., Fu, J.D., Delgado-Olguin, P., Vedantham, V., Hayashi, Y., Bruneau, B.G., and Srivastava, D. (2010). Direct reprogramming of fibroblasts into functional cardiomyocytes by defined factors. Cell *142*, 375–386.

Kattman, S.J., Huber, T.L., and Keller, G.M. (2006). Multipotent flk-1+ cardiovascular progenitor cells give rise to the cardiomyocyte, endothelial, and vascular smooth muscle lineages. Dev. Cell *11*, 723–732.

Kattman, S.J., Witty, A.D., Gagliardi, M., Dubois, N.C., Niapour, M., Hotta, A., Ellis, J., and Keller, G. (2011). Stage-specific optimization of activin/nodal and BMP signaling promotes cardiac differentiation of mouse and human pluripotent stem cell lines. Cell Stem Cell *8*, 228–240.

Kent, D.G., Copley, M.R., Benz, C., Wöhrer, S., Dykstra, B.J., Ma, E., Cheyne, J., Zhao, Y., Bowie, M.B., Zhao, Y., et al. (2009). Prospective isolation and molecular characterization of hematopoietic stem cells with durable self-renewal potential. Blood *113*, 6342–6350.

Kim, I., Saunders, T.L., and Morrison, S.J. (2007). Sox17 dependence distinguishes the transcriptional regulation of fetal from adult hematopoietic stem cells. Cell *130*, 470–483.

Lancrin, C., Sroczynska, P., Stephenson, C., Allen, T., Kouskoff, V., and Lacaud, G. (2009). The haemangioblast generates haematopoietic cells through a haemogenic endothelium stage. Nature *457*, 892–895.

Lee, D., Park, C., Lee, H., Lugus, J.J., Kim, S.H., Arentson, E., Chung, Y.S., Gomez, G., Kyba, M., Lin, S., et al. (2008). ER71 acts downstream of BMP, Notch, and Wnt signaling in blood and vessel progenitor specification. Cell Stem Cell *2*, 497–507.

Lin, C.R., Kioussi, C., O'Connell, S., Briata, P., Szeto, D., Liu, F., Izpisúa-Belmonte, J.C., and Rosenfeld, M.G. (1999). Pitx2 regulates lung asymmetry, cardiac positioning and pituitary and tooth morphogenesis. Nature *401*, 279–282.

Liu, F., Bhang, S.H., Arentson, E., Sawada, A., Kim, C.K., Kang, I., Yu, J., Sakurai, N., Kim, S.H., Yoo, J.J., et al. (2013). Enhanced hemangioblast generation and improved vascular repair and regeneration from embryonic stem cells by defined transcription factors. Stem Cell Rep. *1*, 166–182.

Lu, M.F., Pressman, C., Dyer, R., Johnson, R.L., and Martin, J.F. (1999). Function of Rieger syndrome gene in left-right asymmetry and craniofacial development. Nature *401*, 276–278.

Malynn, B.A., de Alboran, I.M., O'Hagan, R.C., Bronson, R., Davidson, L., DePinho, R.A., and Alt, F.W. (2000). N-myc can functionally replace c-myc in murine development, cellular growth, and differentiation. Genes Dev. *14*, 1390–1399.

Medvinsky, A.L., Samoylina, N.L., Müller, A.M., and Dzierzak, E.A. (1993). An early pre-liver intraembryonic source of CFU-S in the developing mouse. Nature *364*, 64–67.

Mikkola, H.K., and Orkin, S.H. (2006). The journey of developing hematopoietic stem cells. Development *133*, 3733–3744.

Müller, A.M., Medvinsky, A., Strouboulis, J., Grosveld, F., and Dzierzak, E. (1994). Development of hematopoietic stem cell activity in the mouse embryo. Immunity *1*, 291–301.

Nakajima-Takagi, Y., Osawa, M., Oshima, M., Takagi, H., Miyagi, S., Endoh, M., Endo, T.A., Takayama, N., Eto, K., Toyoda, T., et al. (2013). Role of SOX17 in hematopoietic development from human embryonic stem cells. Blood *121*, 447–458.

Nakamura, S., Takayama, N., Hirata, S., Seo, H., Endo, H., Ochi, K., Fujita, K., Koike, T., Harimoto, K., Dohda, T., et al. (2014). Expandable megakaryocyte cell lines enable clinically applicable generation of platelets from human induced pluripotent stem cells. Cell Stem Cell *14*, 535–548.

Nakano, H., Liu, X., Arshi, A., Nakashima, Y., van Handel, B., Sasidharan, R., Harmon, A.W., Shin, J.H., Schwartz, R.J., Conway, S.J., et al. (2013). Haemogenic endocardium contributes to transient definitive haematopoiesis. Nat. Commun. *4*, 1564.

Nishikawa, S.I., Nishikawa, S., Hirashima, M., Matsuyoshi, N., and Kodama, H. (1998). Progressive lineage analysis by cell sorting and culture identifies FLK1+VE-cadherin+ cells at a diverging point of endothelial and hemopoietic lineages. Development *125*, 1747–1757.

Owens, G.K. (1995). Regulation of differentiation of vascular smooth muscle cells. Physiol. Rev. *75*, 487–517.

Pereira, C.F., Lemischka, I.R., and Moore, K. (2012). Reprogramming cell fates: insights from combinatorial approaches. Ann. N. Y. Acad. Sci. *1266*, 7–17.

Pereira, C.F., Chang, B., Qiu, J., Niu, X., Papatsenko, D., Hendry, C.E., Clark, N.R., Nomura-Kitabayashi, A., Kovacic, J.C., Ma'ayan, A., et al. (2013). Induction of a hemogenic program in mouse fibroblasts. Cell Stem Cell *13*, 205–218.

Petriv, O.I., Kuchenbauer, F., Delaney, A.D., Lecault, V., White, A., Kent, D., Marmolejo, L., Heuser, M., Berg, T., Copley, M., et al. (2010). Comprehensive microRNA expression profiling of the hematopoietic hierarchy. Proc. Natl. Acad. Sci. USA *107*, 15443–15448.

Plotnikov, A.N., Schlessinger, J., Hubbard, S.R., and Mohammadi, M. (1999). Structural basis for FGF receptor dimerization and activation. Cell *98*, 641–650.

Riddell, J., Gazit, R., Garrison, B.S., Guo, G., Saadatpour, A., Mandal, P.K., Ebina, W., Volchkov, P., Yuan, G.C., Orkin, S.H., and Rossi, D.J. (2014). Reprogramming committed murine blood cells to induced hematopoietic stem cells with defined factors. Cell *157*, 549–564.

Ruiz-Herguido, C., Guiu, J., D'Altri, T., Inglés-Esteve, J., Dzierzak, E., Espinosa, L., and Bigas, A. (2012). Hematopoietic stem cell development requires transient Wnt/β-catenin activity. J. Exp. Med. *209*, 1457–1468.

Sargent, C.Y., Berguig, G.Y., and McDevitt, T.C. (2009). Cardiomyogenic differentiation of embryoid bodies is promoted by rotary orbital suspension culture. Tissue Eng. Part A *15*, 331–342.

Satoh, Y., Matsumura, I., Tanaka, H., Ezoe, S., Sugahara, H., Mizuki, M., Shibayama, H., Ishiko, E., Ishiko, J., Nakajima, K., and Kanakura, Y. (2004). Roles for c-Myc in self-renewal of hematopoietic stem cells. J. Biol. Chem. *279*, 24986–24993.

Sauvageau, G., Thorsteinsdottir, U., Eaves, C.J., Lawrence, H.J., Largman, C., Lansdorp, P.M., and Humphries, R.K. (1995). Overexpression of HOXB4 in hematopoietic cells causes the selective expansion of more primitive populations in vitro and in vivo. Genes Dev. *9*, 1753–1765.

Shalaby, F., Rossant, J., Yamaguchi, T.P., Gertsenstein, M., Wu, X.F., Breitman, M.L., and Schuh, A.C. (1995). Failure of blood-island formation and vasculogenesis in Flk-1-deficient mice. Nature *376*, 62–66.

Shalaby, F., Ho, J., Stanford, W.L., Fischer, K.D., Schuh, A.C., Schwartz, L., Bernstein, A., and Rossant, J. (1997). A requirement

for Flk1 in primitive and definitive hematopoiesis and vasculogenesis. Cell *89*, 981–990.

Shivdasani, R.A., Mayer, E.L., and Orkin, S.H. (1995). Absence of blood formation in mice lacking the T-cell leukaemia oncoprotein tal-1/SCL. Nature *373*, 432–434.

Silver, L., and Palis, J. (1997). Initiation of murine embryonic erythropoiesis: a spatial analysis. Blood *89*, 1154–1164.

Sturgeon, C.M., Chicha, L., Ditadi, A., Zhou, Q., McGrath, K.E., Palis, J., Hammond, S.M., Wang, S., Olson, E.N., and Keller, G. (2012). Primitive erythropoiesis is regulated by miR-126 via non-hematopoietic Vcam-1+ cells. Dev. Cell *23*, 45–57.

Takada, K., Saito, M., Kaneko, H., Iizuka, K., Kokai, Y., and Fujimoto, J. (1995). Novel monoclonal antibody reactive with thrombin-sensitive 74-kDa glycoproteins present on platelets and megakaryocytes both from mouse and rat. Hybridoma *14*, 361–367.

Takahashi, K., and Yamanaka, S. (2006). Induction of pluripotent stem cells from mouse embryonic and adult fibroblast cultures by defined factors. Cell *126*, 663–676.

Takahashi, K., Tanabe, K., Ohnuki, M., Narita, M., Ichisaka, T., Tomoda, K., and Yamanaka, S. (2007). Induction of pluripotent stem cells from adult human fibroblasts by defined factors. Cell *131*, 861–872.

Taoudi, S., Gonneau, C., Moore, K., Sheridan, J.M., Blackburn, C.C., Taylor, E., and Medvinsky, A. (2008). Extensive hematopoietic stem cell generation in the AGM region via maturation of VE-cadherin+CD45+ pre-definitive HSCs. Cell Stem Cell *3*, 99–108.

Thomson, J.A., Itskovitz-Eldor, J., Shapiro, S.S., Waknitz, M.A., Swiergiel, J.J., Marshall, V.S., and Jones, J.M. (1998). Embryonic stem cell lines derived from human blastocysts. Science *282*, 1145–1147.

Tsai, F.Y., Keller, G., Kuo, F.C., Weiss, M., Chen, J., Rosenblatt, M., Alt, F.W., and Orkin, S.H. (1994). An early haematopoietic defect in mice lacking the transcription factor GATA-2. Nature *371*, 221–226.

Vallier, L., Alexander, M., and Pedersen, R.A. (2005). Activin/Nodal and FGF pathways cooperate to maintain pluripotency of human embryonic stem cells. J. Cell Sci. *118*, 4495–4509.

Vodyanik, M.A., Yu, J., Zhang, X., Tian, S., Stewart, R., Thomson, J.A., and Slukvin, I.I. (2010). A mesoderm-derived precursor for mesenchymal stem and endothelial cells. Cell Stem Cell *7*, 718–729.

Wang, L., Schulz, T.C., Sherrer, E.S., Dauphin, D.S., Shin, S., Nelson, A.M., Ware, C.B., Zhan, M., Song, C.Z., Chen, X., et al. (2007). Self-renewal of human embryonic stem cells requires insulin-like growth factor-1 receptor and ERBB2 receptor signaling. Blood *110*, 4111–4119.

Warren, A.J., Colledge, W.H., Carlton, M.B., Evans, M.J., Smith, A.J., and Rabbitts, T.H. (1994). The oncogenic cysteine-rich LIM domain protein rbtn2 is essential for erythroid development. Cell *78*, 45–57.

Weng, W., and Sheng, G. (2014). Five Transcription Factors and FGF Pathway Inhibition Efficiently Induce Erythroid Differentiation in the Epiblast. Stem Cell Rep. *2*, 262–270.

Xiao, Q., Zeng, L., Zhang, Z., Hu, Y., and Xu, Q. (2007). Stem cell-derived Sca-1+ progenitors differentiate into smooth muscle cells, which is mediated by collagen IV-integrin alpha1/beta1/alphav and PDGF receptor pathways. Am. J. Physiol. Cell Physiol. *292*, C342–C352.

Xu, R.H., Peck, R.M., Li, D.S., Feng, X., Ludwig, T., and Thomson, J.A. (2005). Basic FGF and suppression of BMP signaling sustain undifferentiated proliferation of human ES cells. Nat. Methods *2*, 185–190.

Yamashita, J., Itoh, H., Hirashima, M., Ogawa, M., Nishikawa, S., Yurugi, T., Naito, M., Nakao, K., and Nishikawa, S. (2000). Flk1-positive cells derived from embryonic stem cells serve as vascular progenitors. Nature *408*, 92–96.

Yao, H., Liu, B., Wang, X., Lan, Y., Hou, N., Yang, X., and Mao, N. (2007). Identification of high proliferative potential precursors with hemangioblastic activity in the mouse aorta-gonad- mesonephros region. Stem Cells *25*, 1423–1430.

Yu, J., Vodyanik, M.A., Smuga-Otto, K., Antosiewicz-Bourget, J., Frane, J.L., Tian, S., Nie, J., Jonsdottir, G.A., Ruotti, V., Stewart, R., et al. (2007). Induced pluripotent stem cell lines derived from human somatic cells. Science *318*, 1917–1920.

Zhang, H.Z., Degar, B.A., Rogoulina, S., Resor, C., Booth, C.J., Sinning, J., Gage, P.J., and Forget, B.G. (2006). Hematopoiesis following disruption of the Pitx2 homeodomain gene. Exp. Hematol. *34*, 167–178.

Zhang, J., Liu, J., Huang, Y., Chang, J.Y., Liu, L., McKeehan, W.L., Martin, J.F., and Wang, F. (2012). FRS2α-mediated FGF signals suppress premature differentiation of cardiac stem cells through regulating autophagy activity. Circ. Res. *110*, e29–e39.

Stem Cell Reports, Volume *3*
Supplemental Information

An Expandable, Inducible Hemangioblast State Regulated by Fibroblast Growth Factor

David T. Vereide, Vernella Vickerman, Scott A. Swanson, Li-Fang Chu, Brian E. McIntosh, and James A. Thomson

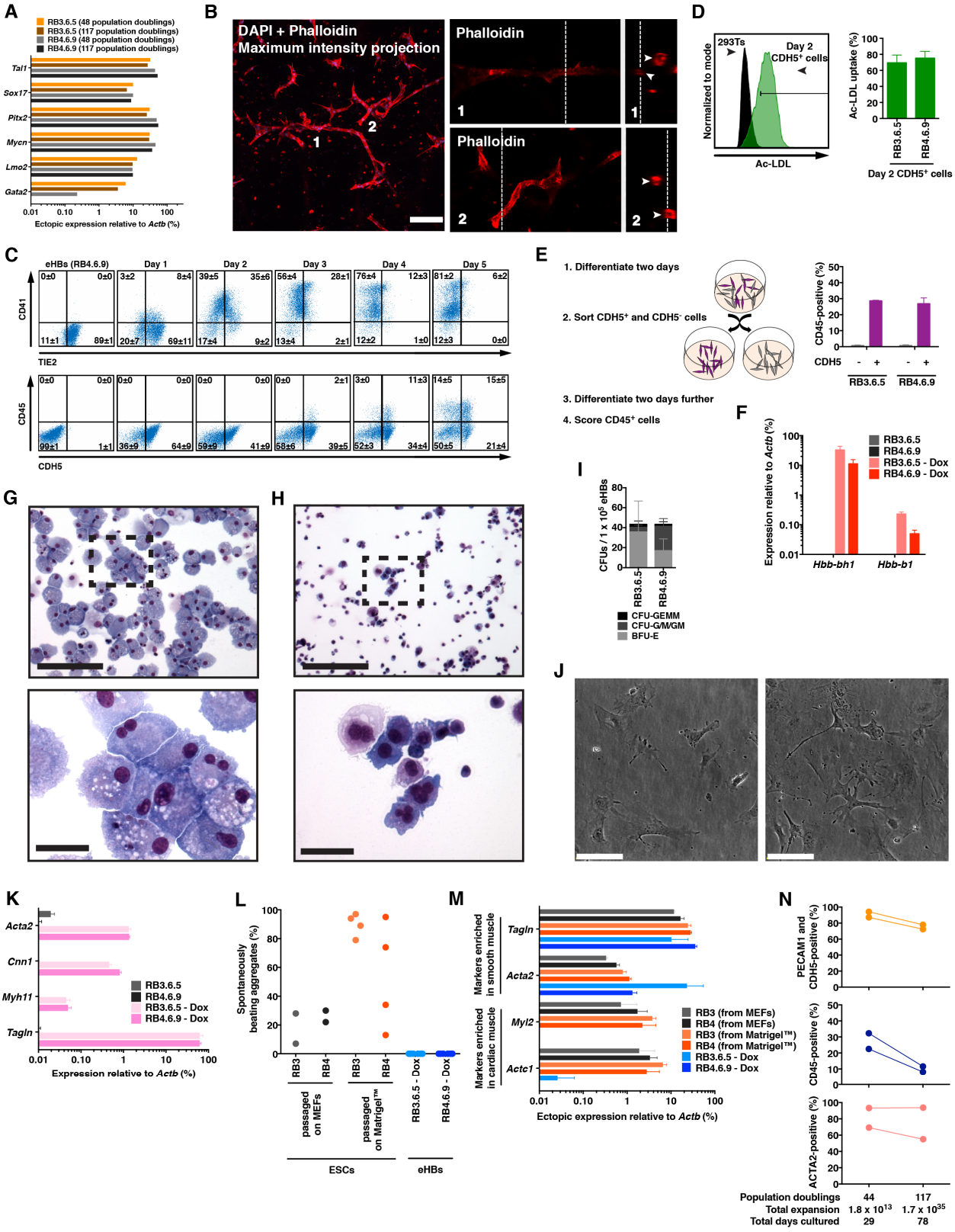
A
RB3.6.5 (48 population doublings)
RB3.6.5 (117 population doublings)
RB4.6.9 (48 population doublings)
RB4.6.9 (117 population doublings)
Tal1
Sox17
Pitx2
Mycn
Lmo2
Gata2
Ectopic expression relative to Actb (%)
B
DAPI + Phalloidin
Maximum intensity projection
Phalloidin
Phalloidin
D
293Ts
Day 2 CDH5+ cells
Normalized to mode
Ac-LDL
Ac-LDL uptake (%)
RB3.6.5
RB4.6.9
Day 2 CDH5+ cells
C
eHBs (RB4.6.9)
Day 1
Day 2
Day 3
Day 4
Day 5
CD41
TIE2
CD45
CDH5
E
1. Differentiate two days
2. Sort CDH5+ and CDH5- cells
3. Differentiate two days further
4. Score CD45+ cells
CD45-positive (%)
CDH5
RB3.6.5
RB4.6.9
F
Expression relative to Actb (%)
RB3.6.5
RB4.6.9
RB3.6.5 - Dox
RB4.6.9 - Dox
Hbb-bh1
Hbb-b1
I
CFUs / 1 x 10^5 eHBs
RB3.6.5
RB4.6.9
CFU-GEMM
CFU-G/M/GM
BFU-E
G
H
J
K
Acta2
Cnn1
Myh11
Tagln
RB3.6.5
RB4.6.9
RB3.6.5 - Dox
RB4.6.9 - Dox
Expression relative to Actb (%)
L
Spontaneously beating aggregates (%)
RB3
RB4
RB3
RB4
RB3.6.5 - Dox
RB4.6.9 - Dox
passaged on MEFs
passaged on Matrigel™
ESCs
eHBs
M
Markers enriched in smooth muscle
Markers enriched in cardiac muscle
Tagln
Acta2
Myl2
Actc1
RB3 (from MEFs)
RB4 (from MEFs)
RB3 (from Matrigel™)
RB4 (from Matrigel™)
RB3.6.5 - Dox
RB4.6.9 - Dox
Ectopic expression relative to Actb (%)
N
PECAM1 and CDH5-positive (%)
CD45-positive (%)
ACTA2-positive (%)
Population doublings 44 117
Total expansion 1.8 x 10^13 1.7 x 10^35
Total days cultured 29 78

Figure S1, related to Figure 2: Characterization of the expandable hemangioblasts
(A, F, K, M) Measurements of gene expression by qPCR, normalized to *Actb*. The y-axis is on a $\log_{10}$ scale, with a threshold of detection cutoff of 0.01%. (A) Ectopic gene expression in two eHB lines. Estimated population doublings are based on the average doubling time (16 hours) as determined in Figure 5B. (B) Lumenized tubes. Cultured as described in Figure 2C except cells were embedded in Matrigel™ for 20 days. The left image is a maximum intensity projection of a Z-stack of images, viewed along the X-Y plane. White bar = 100 μm. The numbers indicate regions of interest that correspond to the images in the middle, which are of a single Z position viewed along the X-Y plane. The dashed lines in the middle images indicate the position of the corresponding images on the right, which are the projected image viewed from the Y-Z plane. The arrows point to lumen. (C) Hematopoietic differentiation timecourse conducted and depicted as described in Figure 2D, except that here the eHB line RB4.6.9 is employed. (D, E) Further analysis of the CDH5-positive cells arising two days after the withdrawal of doxycycline, as described in Figure 2D and S1C. (D) Measurement of the ability of the cells to take up acetylated LDL. Left, an example histogram. 293T cells served as a negative control. The bar indicates the cells considered positive for Ac-LDL uptake. Note the bar is different from the bar used in Figure 2B to measure "efficient" uptake. In contrast, the bar employed here measures total uptake. Right, the average percent of cells ± S.D. taking up acetylated LDL from two independent experiments of each line. (E) Left, experimental design. eHBs were differentiated as in (C) for two days and then sorted based on their CDH5 expression by FACS (gated conservatively to ensure high purity). Sorted CDH5-positive or CDH5-negative cells were cultured for two days further, and then the percentage of cells positive for CD45 in each population was determined by FACS. Right, the average percent of cells ± S.D from two independent experiments of each line. (F) Measurements of the expression of hemoglobin in cells described in Figure 2E by qPCR. Results are the average expression ± S.D from three independent experiments of each line. (G, H) Giemsa staining of unsorted differentiated blood cells from the eHB line RB3.6.5. The boxed areas in the top images are shown below at higher magnification. Top image black bars = 200 μm. Bottom image black bars = 40 μm. (G) Macrophages differentiated for nine days. (H) Megakaryocytes differentiated for four days. (I) Hematopoietic colony forming units (CFUs) formed in methylcellulose (M3434, StemCell Technologies). Results are the average efficiency ± S.D from three independent experiments of each line. (J) Example images of smooth muscle cells differentiated as described in Figure 2H. Cells derived from the eHB line RB3.6.5 are shown on the left; cells derived from the eHB line RB4.6.9 are shown on the right. White bars = 100 μm. (K) Measurements of the expression level of smooth muscle markers in cells described in Figure 2H by qPCR. Results are the average expression ± S.D from three independent experiments of each line. (L) Quantification of spontaneously beating aggregates. A total of six experiments were performed, two with control ESCs that had been passaged on MEFs, and four with control ESCs that had been briefly passaged on Matrigel™. There were surviving aggregates from the eHB line RB4.6.9 in all six experiments to score. There were surviving aggregates from the eHB line RB3.6.5 in only two experiments (survival correlated positively with passage number), in the remaining four experiments they died out before the end of the assay. (M) Measurements of the expression level of smooth and cardiac muscle markers by qPCR of cultures from (L). Results are the average expression ± S.D from at least two independent experiments of each line. (N) Analysis of the endothelial (top graph, three days differentiation), blood (middle graph, four days differentiation), or smooth muscle (bottom graph, three days differentiation) potential of two independent eHB lines (RB3.6.5 and RB4.6.9) as determined by the indicated markers. Cells were tested for their ability to give rise to these cell types after culturing for the indicated lengths in Vm containing doxycycline. Assays were conducted as described in Figure 1 or 2. Estimated population doublings and total expansion values are based on the average doubling time (16 hours) as determined in Figure 5B.

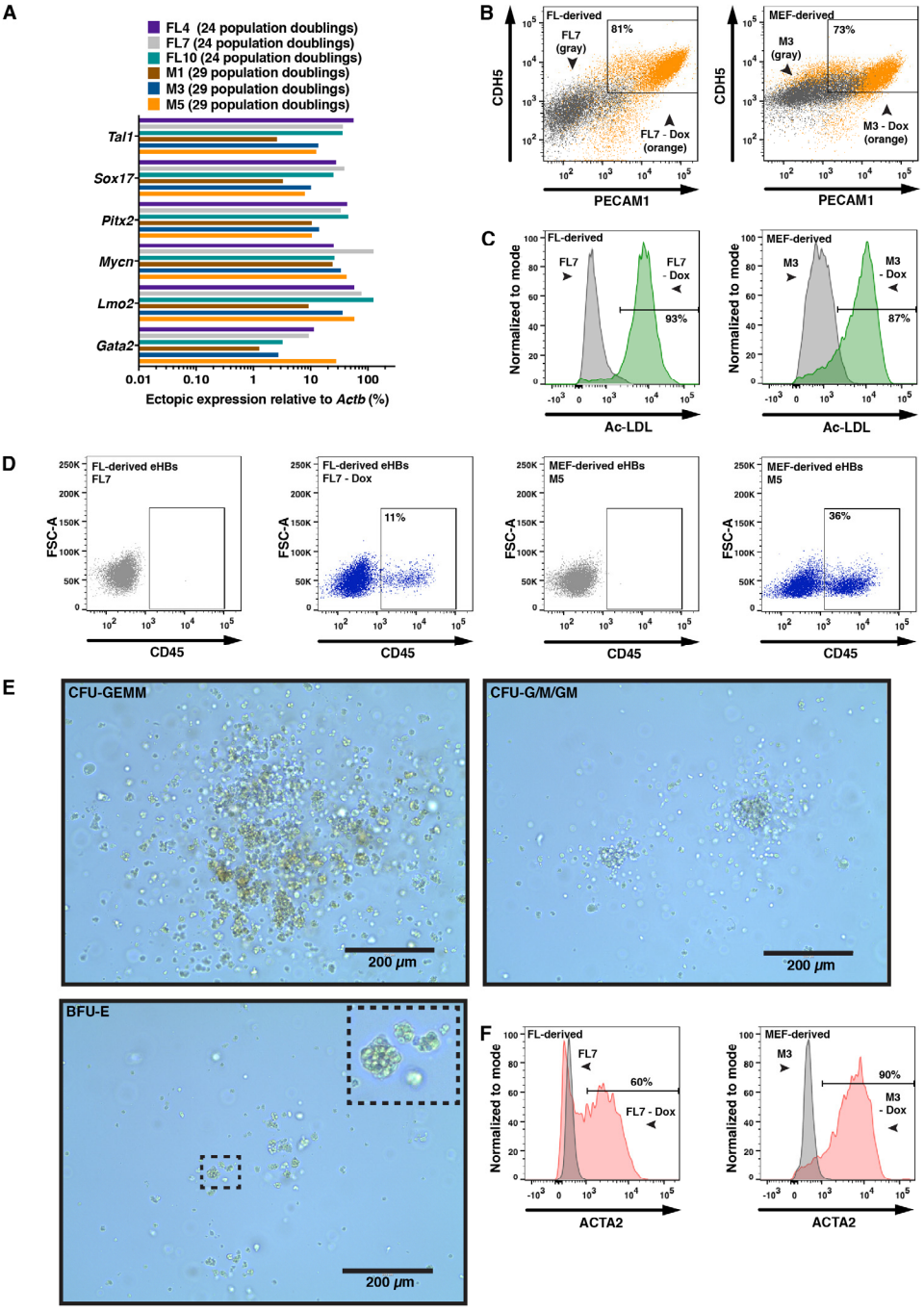

Figure S2, related to Figure 3: The eHBs can be derived from different cell sources
(A) Measurements of ectopic gene expression in six eHB lines by qPCR, normalized to *Actb*. The y-axis is on a $\log_{10}$ scale. Estimated population doublings are based on the average doubling time (16 hours) as determined in Figure 5B. (B, C, D, F) Example FACS dot plots or histograms of FL- or MEF- derived eHBs and their differentiated progeny ("- Dox"). Refer to Figure 3 to see the compiled results from all the tested lines. The eHB lines FL7 and M3 are presented because they tended to

form the median among the lines, except (D) in which M5, the only MEF-derived eHB to appreciably generate CD45-positive cells, is shown. The percentage of differentiated cells considered positive in each assay is shown. Assays were conducted as described in Figure 1 or 2. (B, C) Endothelial assays (three days differentiation). (D) Blood assays (four days differentiation). (E) Example blood colonies derived from the eHB line FL10. Images taken six days after plating in methylcellulose (nine days after the withdrawal of doxycycline). In the lower image, the small dotted box indicates the location of the inset, zoomed in. (F) Smooth muscle assays (three days differentiation).

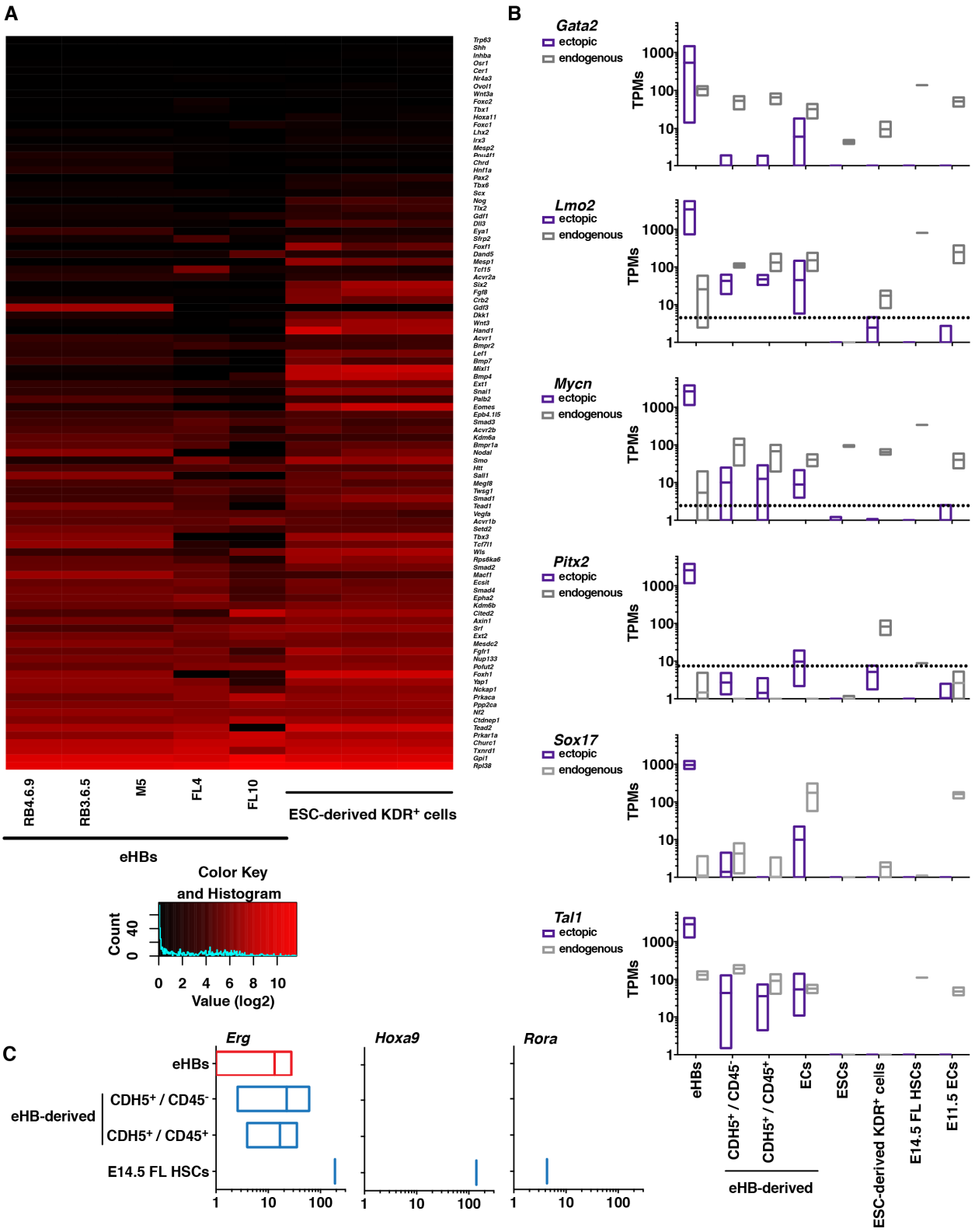
A
RB4.6.9
RB3.6.5
M5
FL4
FL10
ESC-derived KDR+ cells
eHBs
Color Key and Histogram
Count
Value (log2)
B
Gata2
Lmo2
Mycn
Pitx2
Sox17
Tal1
ectopic
endogenous
TPMs
eHBs
CDH5+ / CD45-
CDH5+ / CD45+
ECs
ESCs
ESC-derived KDR+ cells
E14.5 FL HSCs
E11.5 ECs
eHB-derived
C
Erg
Hoxa9
Rora
eHBs
eHB-derived
CDH5+ / CD45-
CDH5+ / CD45+
E14.5 FL HSCs

Figure S3, related to Figure 4: RNA-seq uncovers the developmental state of the eHBs
The data are compiled from the RNA-seq experiments performed in Figure 4. (A) Heatmap of genes associated with mesoderm development. Represented as the $\log_2$ values of the TPM measurements. (B, C) Expression levels of genes. The box sizes represent the minimum to maximum values, with the mean depicted as a horizontal line within each box. The y-axes are on a $\log_{10}$ scale, with a threshold of detection cutoff of 1 TPM. (B) The six transcription factors either ectopically or endogenously expressed. The horizontal dotted lines provide a measure of the background noise: the extent to which the algorithm (RSEM) apparently fails to distinguish endogenous from ectopic transcripts, as noted by the presence of ectopic signals in cells that do not express the ectopic genes (the four cell types furthest to the right). (C) Hematopoietic factors key to the ability to generate CFUs.

eHB cell line	Origin	Gender	Passage number	Abnormal clone(s) detected	Frequency	Associated figures
RB2.6.3	ESC	Male	5	XO	5 of 22 cells	Not characterized in detail
RB2.6.6	ESC	Male	6	XO	2 of 20 cells	Not characterized in detail
				XYY	2 of 20 cells	
RB3.6.5	ESC	Male	6	None detected	-	Figure 2, 4, 5, S1, S3
			9	XYY	2 of 22 cells	
RB3.6.10	ESC	Male	5	XYY	2 of 20 cells	Not characterized in detail
RB4.6.9	ESC	Male	7	None detected	-	Figure 2, 4, 5, S1, S3
RB4.6.3	ESC	Male	5	XO	4 of 20 cells	Not characterized in detail
M1	MEF	Female	9	Trisomy 2	4 of 20 cells	Figure 3, S2
M3	MEF	Male	9	XYY	20 of 20 cells	Figure 3, S2
M5	MEF	Female	9	None detected	-	Figure 3, 4, S2, S3
FL4	Fetal liver	Female	6	None detected	-	Figure 3, 4, 5, S2, S3
FL7	Fetal liver	Male	7	None detected	-	Figure 3, 4, 5, S2
FL10	Fetal liver	Male	7	None detected	-	Figure 3, 4, 5, S2, S3

Table S1, related to Figure 2, 3, 4, 5
The karyotypes of example eHB lines, with the threshold of detection of an abnormal clone defined as two or more analyzed cells exhibiting the same abnormality. The passage number indicates when the cells were analyzed.

Movie S1, Related to Figure 5: The effect of fibroblast growth factor on the eHBs. Cells were maintained with doxycycline in Vm. Cells were observed for 48 hours and images were taken every 30 minutes. The yellow line corresponds to 0.10 mm. The eHB line RB3.6.5 is presented.

Movie S2, Related to Figure 5: The effect of fibroblast growth factor on the eHBs. Cells were maintained with doxycycline in N2B27 medium without any additional growth factors. Cells were observed for 48 hours and images were taken every 30 minutes. The yellow line corresponds to 0.10 mm. The eHB line RB3.6.5 is presented.

Movie S3, Related to Figure 5: The effect of fibroblast growth factor on the eHBs. Cells were maintained with doxycycline in N2B27 medium supplemented with FGF2. Cells were observed for 48 hours and images were taken every 30 minutes. The yellow line corresponds to 0.10 mm. The eHB line RB3.6.5 is presented.

SUPPLEMENTAL EXPERIMENTAL PROCEDURES

Mice, mES isolation and culture, MEF isolation and culture

The B6.SJL-*Ptprc*^{a} *Pepc*^{b}/BoyJ (Jackson, stock number 002014) mice were intercrossed with the B6.Cg-*Gt(ROSA)26Sor*$^{tm1(rtTA*M2)Jae}$/J (Jackson, stock number 006965) mouse strain to obtain progeny (referred to here as RosaBoy) homozygous for both the CD45.1 allele and the R26-M2rtTA allele. RosaBoy females and males were time mated (the morning of the day a vaginal plug was discovered was considered embryonic day 0.5). Embryos were obtained on embryonic day 3.5 from pregnant females, and embryonic stem cells were isolated and expanded from them, following a procedure adapted from previous reports (Bryja et al., 2006; Chu et al., 2011). Three independent embryonic stem cell lines, RB2, RB3, and RB4, were expanded in culture and verified to be free of clonal karyotypic abnormalities (Wicell). They were maintained in culture on irradiated mouse embryonic fibroblast feeders in Knockout DMEM (Life Technologies) supplemented with 10% FBS (StemCell, catalog number 06952), non-essential amino acids (Life Technologies), GlutaMAX™ (Life Technologies), 100 µM -mercaptoethanol (Life Technologies), 3 µM CHIR99021 (Stemgent), 1 µM PD0325901 (Stemgent), and 1000 U/mL LIF (Millipore). Mouse embryonic fibroblasts (MEFs) for reprogramming were derived from embryonic day 12.5 embryos of the B6.Cg-*Gt(ROSA)26Sor*$^{tm1(rtTA*M2)Jae}$/J (Jackson, stock number 006965) strain and cultured in MEF medium [DMEM supplemented with 10% FBS (Hyclone) and non-essential amino acids].

Differentiation of murine ES cells to hemogenic endothelium

Conducted as previously described (Chiang and Wong, 2011). Murine ES cells were cultured for two days in Matrigel™ (BD)-coated plasticware in N2B27 medium [50% N-2 medium (Neurobasal® medium and N-2 supplement), 50% B-27 medium (DMEM/F12 and B-27® supplement, minus vitamin A), non-essential amino acids, GlutaMAX™, 100 µM -mercaptoethanol, and 25 µg/mL BSA fraction V, all reagents from Life Technologies]. The medium was then changed to N2B27 medium supplemented with 4 ng/mL Activin A (R&D Systems), 3 µM CHIR99021 (Stemgent), 5 ng/mL human BMP4 (R&D Systems), and 12.5 ng/mL human FGF2 (synthesized and purified in our lab). After two additional days, cells were replated in Vm [N2B27 medium supplemented with 20 ng/mL murine VEGF (R&D Systems or Peprotech), 250 µM 8-Bromoadenosine 3•,5•-cyclic monophosphate sodium salt (Sigma), 4 µM SB431542 (Sigma or Cellagen), 20 ng/mL human BMP4, and 12.5 ng/mL human FGF2], and cultured further. When performing assays with introduced doxycycline inducible factors, the same procedure was followed, except the ES cells were electroporated as described below prior to plating in N2B27 medium, and 2 µg/mL doxycycline (Sigma) was added to Vm to activate gene expression in the ESC-derived mesoderm cells (day four of the differentiation).

Electroporation

Murine ES cells, embryonic fibroblasts [either cell type dissociated with TypLE (Life Technologies)] or fetal liver cells were suspended N2B27 medium supplemented with 25 mM HEPES. Depending on the cell type, 2-10 x 10^5 cells in 0.5 mL medium were mixed with 30 µg DNA (purified using the HiSpeed Plasmid Maxi Kit, Qiagen) and 1 µg hyPBase mRNA (Yusa et al., 2011) (synthesized using mMESSAGE mMACHINE T7 Ultra Kit, Life Technologies from a PCR product encoding the T7 promoter, hyPBase, and BGH polyA sequences). Cells were then placed in 0.4 cm cuvettes (Biorad) and electroporated with Gene Pulser II (Biorad) at 250 volts, 500-1000 µFarads, and infinite resistance.

Induction of eHBs from MEFs or fetal liver cells
B6.Cg-*Gt(ROSA)26Sor*$^{tm1(rtTA*M2)Jae}$/J MEFs and RosaBoy fetal liver (FL) cells were employed. Total fetal liver cells were obtained from day 14.5 embryos as described below, except that they were unsorted. Both MEF and primary FL cells were electroporated as described above and placed on Matrigel™ -coated plasticware. The MEFs were cultured in MEF medium containing 2 µg/mL doxycycline and the fetal liver cells were cultured in Stemline II (Sigma) supplemented with 100 ng/mL SCF, 100 ng/mL IL-3 (R&D Systems or Peprotech), and 2 µg/mL doxycycline. The cells were gradually transitioned to N2B27 medium containing 12.5 ng/mL FGF2 and 2 µg/mL doxycycline (BFD) over the following days by removing about half the medium each day and replacing it with fresh BFD.

Quantitative PCR (qPCR) analysis
Total RNAs were purified using RNeasy kits (Qiagen) with either on-column DNAse treatment or genomic DNA removal columns, and the purified RNAs were reverse transcribed with SuperScript VILO (Life Technologies). TaqMan® realtime qPCR reactions (20 µL total volumes) were performed in wells containing TaqMan® Universal Master Mix II with or without UNG (Life Technologies), 1 µL of the cDNA reaction, and 1 µL of the following primer/probe sets (all from Life Technologies): Mm00607939_s1 (*Actb*), Mm01611268_g1 (*Hbb-b1*), Mm00433932_g1 (*Hbb-bh1*), Mm00487032_m1 (*Cnn1*), Mm00725412_s1 (*Acta2*), Mm00441661_g1 (*Tagln*), Mm00443013_m1 (*Myh11*), Mm01333821_M1 (*Actc1*), and Mm00440384_M1 (*Myl2*).
SYBR® Green realtime qPCR reactions (also 20 µL total volumes) were performed in wells containing 1X *Power* SYBR® Green master mix (Life Technologies), 1 µL of the cDNA reaction and 0.3 µM of the following primers listed below. The expression levels of the ectopic genes were detected using a common reverse primer complementary to the vector sequence and a forward primer complementary to the particular gene sequence. The *Actb* primer sequences have been previously reported (Pathak et al., 2014).

Gene	Primer	Sequence (5` to 3`)
Actb	Forward	CCA CCA TGT ACC CAG GCA TT
Actb	Reverse	AGG GTG TAA AAC GCA GCT CA
Ectopic factor	Reverse	GCT CTA GAG TCG GTG ACT AGT AT
Gata2	Forward	CCT CCT CCA GTC TCT CCT TT
Lmo2	Forward	CCT TCT CAT CAA CTC CGA CAT AG
Mycn	Forward	CAG CAG CAG TTG CTA AAG AAG
Pitx2	Forward	CCT GAG TGC TTG CCA GTA T
Sox17	Forward	TCG AAC AGT ATC TGC CCT TTG
Tal1	Forward	CTC CAT CCT GCC CTG CT

Reaction signals were measured on a ViiA 7 (Life Technologies) and analyzed by the ViiA 7 v1.1 - v1.2.3 software. When normalizing signals to *Actb*, the amplification efficiency was assumed to be

100% (e.g. 1 CT = 2 fold increase). The expression level of each gene was then described as a percentage of the expression level of *Actb*.

Small molecule inhibitors
The following small molecules were employed: PD173074 (Mohammadi et al., 1998) (Stemgent), PI828 (Gharbi et al., 2007) (Tocris), PD0325901 (Barrett et al., 2008) (Stemgent), U0126 (Favata et al., 1998) (Sigma). All were dissolved in DMSO and used at the concentrations indicated in Figure 5.

Endothelial differentiation of eHBs
Cells were dissociated by incubation and trituration in HEH [0.5 mM EDTA (Fisher) in 1x HBSS supplemented with 10 mM HEPES (both from Life Technologies)] and replated at 1 x 10^5/10 cm^2 on Matrigel™ -coated plasticware in Vm and cultured for three days. To form capillary-like networks, cells were plated at 1.5 x 10^6/60 cm^2 in Vm for seven days and then dissociated and embedded in Matrigel™ (4.6 mg/mL, BD, 354230) at a concentration of 10 x 10^6 cells/mL. The three-dimensional (3D) Matrigel™/cell constructs were formed in µ-Slide Angiogenesis wells (Ibidi, 81506). The 3D constructs were cultured in Vm supplemented additionally with 50 ng/mL murine VEGF and human FGF2 for ten or twenty days and then fixed in paraformaldehyde and stained with Alexa Fluor® 568 Phalloidin (Life Technologies, A12380) and DAPI.

Blood differentiation of eHBs
All experiments were conducted at 1.5% O_2 in a hypoxic glove box (Coy Labs) unless otherwise specified. Cells were dissociated by incubation and trituration in HEH and replated at 0.5-1 x 10^5/10 cm^2 on Matrigel™ -coated plasticware. To generate CD45-positive cells, or for the hematopoietic differentiation timecourses in Figure 2D or S1C, eHBs were placed in N2B27 medium supplemented with SCIF [3 µM CHIR99021 (Stemgent), 100 ng/mL murine SCF, 100 ng/mL murine IL-3, 100 ng/mL murine FLT3L (the latter three from R&D Systems or Peprotech) (Ruiz-Herguido et al., 2012; Taoudi et al., 2008)] (SCIF medium) for four days unless otherwise noted. For erythrocyte differentiation, a previously established protocol was adapted (Sturgeon et al., 2012). Cells were placed in N2B27 medium supplemented with 5 ng/mL murine VEGF (R&D Systems or Peprotech), 3 µM CHIR99021, 1 ng/mL Activin A (R&D Systems), 1 ng/mL human BMP4 (R&D Systems), and 50 µg/mL ascorbic acid (Sigma) for two days. The medium was then changed to N2B27 medium supplemented with 5 ng/mL murine VEGF, 1 ng/mL Activin A, 1 ng/mL human BMP4, 50 µg/mL ascorbic acid, and 100 ng/mL murine EPO (R&D Systems) and cells were cultured for two additional days. For macrophage differentiation, portions of a previously reported protocol were employed (Choi et al., 2011). Cells were differentiated as described above in SCIF medium for three days, then transferred to N2B27 medium supplemented with 200 ng/mL GM-CSF (Peprotech) on low adherence plates (StemCell Technologies) and cultured for two days at 21% (atmospheric) O_2, and finally transferred to gelatinized plates in IMDM (Life Technologies) supplemented with 10% FBS (Hyclone), 10 ng/mL IL-1 (R&D Systems) and 20 ng/mL M-CSF (Peprotech) and cultured for four days at 21% O_2. For megakaryocyte differentiation, cells were placed in Stemline II medium (Sigma) supplemented with SCIF and 100 ng/mL murine TPO (Peprotech or R&D) and cultured for two days. The medium was then replaced with Stemline II medium containing the same supplements except for CHIR99021, and the cells were cultured for two additional days. Giemsa stains (GS500, Sigma) were performed following the manufacturer's instructions on slides prepared using a Cytospin™ 2 (Shandon). For CFU-C assays, cells growing sub-confluently were placed in N2B27 medium (fetal liver- or MEF-derived lines) or Stemline II medium (ES- or MEF-derived lines) supplemented with SCIF and cultured for three days. Cells were pelleted and gently resuspended in methylcellulose medium (M3434, StemCell Technologies), cultured for three days at 1.5% O_2, and then transferred to 21% O_2. Colonies were scored six days after plating in methylcellulose.

Smooth muscle differentiation of eHBs
Cells were dissociated by incubation and trituration in HEH and replated at 5 x 10^5/10 cm^2 on plasticware coated with 5 µg/10 cm^2 murine collagen IV (Fisher Scientific) in smooth muscle medium

[MEM supplemented with GlutaMAX™, 50 μM -mercaptoethanol (all from Life Technologies), and 10% FBS (Hyclone)], conditions adapted from a previously described protocol (Xiao et al., 2007).

Cardiomyocyte differentiation of ESCs and eHBs
Two previously described protocols were combined and adapted (Sargent et al., 2009; Zhang et al., 2012). The ESCs employed for these assays were either maintained on MEFs as described above or briefly passaged (four to six days) on Matrigel™ in N2B27 medium supplemented with 3 μM CHIR99021, 1 μM PD0325901 and 1000 U/mL LIF, to remove MEF feeders in a manner akin to a previous report (Chiang and Wong, 2011). Cells were dissociated and plated in AggreWell™ plates (StemCell Technologies) at 1000 cells/microwell (except for the ESCs passaged on MEFs, which were plated at 300 cells/microwell) in DMEM supplemented with 10% FBS (StemCell Technologies) and GlutaMAX™. The eHB cultures additionally contained 2 μg/mL doxycycline for the first four days of the protocol. Cells were cultured in the AggreWell™ plates for two days and then the resulting aggregates were gently transferred to low adherence plates (StemCell Technologies) and cultured on a Nutator mixer (24 to 25 RPM, BD) for another four days. The aggregates were then plated on gelatinized plates in the same differentiation medium as above but now additionally supplemented with 100 nM PD173074 and cultured for four more days. Aggregates were scored and lysed ten days from the start of the protocol.

FACS analysis and cell sorting
Cells were stained in cold HBSS+ [1x HBSS (Life Technologies), 2% FBS (HyClone), and 10 mM HEPES (Life Technologies)]. Protocols using this staining buffer can be found at https://www.bcm.edu/research/labs/goodell/index.cfm?PMID=17588. All antibodies, which recognize murine epitopes, were used at a working dilution of 1:100, unless otherwise stated. The following antibodies were purchased from eBioscience: anti-CD42D-APC (17-0421-80), anti-CD71-PE (12-0711-83), anti-TER119-FITC (11-5921), anti-TIE2-PE (12-5987-83), anti-CD16/32 (14-0161-85), anti-CD11B-PE/Cy7 (25-0112-82), and anti-CDH5-biotin (13-1441-80 or -82) [along with streptavidin-PE (12-4317-87)]. The following antibodies were purchased from BD: anti-PECAM1-APC (561814), anti-CD45-FITC (553080), and anti-CDH5-PE (562243). The following antibodies were purchased from Biolegend: anti-CD150-PE/Cy7 (115914), anti-CD41-FITC (133904), anti-CD45.1-APC (110714), and anti-CD48-APC (103412). The following antibodies were purchased from StemCell Technologies: anti-CD201-PE (60038PE) and anti-CD45-FITC (10709). An anti-KDR-APC antibody (used at a 1:20 dilution) was purchased from R&D (FAB4432A). An anti-ACTA2-FITC antibody was purchase from Sigma (F3777). The expression of CDH5 on the emerging blood progeny of the eHBs is low (Figure 2D, S1C), thus for assays with these cells we find that the use of the biotinylated CDH5 antibody coupled to streptavidin-PE, in a manner similar to a previous report (Rybtsov et al., 2011), gives an improved separation of the positive and negative cells in contrast to the antibody directly conjugated to PE. To measure acetylated LDL uptake, cells were incubated for two hours with acetylated LDL conjugated to Alexa Fluor® 488 (Life Technologies). Live stained cells were resuspended for analysis or sorting in HBSS+ with either propidium iodide or DAPI for the exclusion of dead cells. To stain for ACTA2, a protocol for intracellular staining was adapted from one previously described (Xie et al., 2013). The cells were fixed in 4% paraformaldehyde in PBS at 37C for at least 30 minutes, washed with HBSS+, permeabilized in ice-cold 90% methanol for at least one hour, and then blocked and stained in HBSS+ with anti-ACTA2-FITC. Cells were examined on either a FACSAria IIIu or a FACSCanto II (BD) and analyzed using FACSDiva software version 6.1.3 (BD) and FlowJo (Tree Star) software version 9.5.1 and version X 10.0.7r2. Cells were sorted on the FACSAria IIIu. Controls for fluorescence compensation and FACS gating included cells stained with single fluorochromes, and to serve as negative controls, stained cells known to not express the marker(s), such as 293T cells or the parental cell lines.

Fetal liver HSC isolations
Fetal liver HSCs were obtained by a procedure adapted from a previous report (Kent et al., 2009). Embryonic day 14.5 fetal livers from B6.SJL-*Ptprc*^{a} *Pepc*^{b}/BoyJ mice were dissected on ice in

HBSS+ and dissociated by gently mashing through a 40 µm filter (BD). Prior to staining, the non-specific binding of antibodies was blocked by incubating cells on ice in HBSS+ with rat serum (diluted 1:100) and anti-mouse CD16/32 (diluted 1:1000). Cells were then stained on ice in HBSS+ with anti-CD150-PE/Cy7 and subsequently with anti-Cy7 microbeads (Miltenyi Biotec). Cells bound by the microbeads were positively selected using an AutoMACS Pro (Miltenyi Biotec). These cells were then additionally stained on ice with anti-CD201-PE, anti-CD45-FITC, and anti-CD48-APC. Fetal liver HSCs, defined as $CD150^{+}/CD201^{+}/CD48^{-}/CD45^{+}$ were then sorted by FACS into Trizol (Life Technologies) for analysis by RNA-seq.

Primary endothelial cell isolations

Embryos of B6.SJL-*Ptprc*^{a} *Pepc*^{b}/BoyJ mice were isolated on embryonic day 11.5, along with their yolk sacs. The embryos or yolk sacs were dissociated in 0.25% collagenase (dissolved in HBSS supplemented with 20% FBS and 10 mM HEPES) at 37C for 25-30 minutes, triturated, and then passed through a 40 µm filter (BD) to yield single cell suspensions, a process adapted from a previously described protocol (Morgan et al., 2008). The cells were stained on ice in HBSS+ with anti-CDH5-PE and anti-PECAM1-APC. Populations enriched for endothelial cells were defined as $CDH5^{+}/PECAM1^{+}$, and these cells were sorted by FACS into Trizol for analysis by RNA-seq.

RNA-seq preparation, sequencing, and analysis

The murine ESC lines were depleted of MEF feeders by culture on Matrigel™ for four days as described above in “Cardiomyocyte differentiation of ESCs and eHBs.” Total RNAs were purified from Trizol (Life Technology) over RNeasy columns (Qiagen) with DNAse treatment. To make cDNA libraries for sequencing, at least 10 ng of total RNA was reverse transcribed and prepared for sequencing using the Tru-seq RNA Sample Prep kit v2 (Illumina) following the manufacturer's instructions, including the recommended 15 cycles of PCR for amplification. The cDNA libraries were sequenced on an Illumina HiSeq 2500. Base pairs were called by the software Casava v1.8.2 (Illumina). Reads were mapped to a mm10-based transcriptome reference, using the software Bowtie v0.12.9 (Langmead et al., 2009). The reference included all Refseq mRNA transcripts annotated with “NM_” identifiers, augmented with mitochondrial transcripts, hand-selected ENSEMBL transcripts for *Gata2*, *Lmo2*, *Mycn*, *Pitx2*, *Sox17*, and *Tal1* and the predicted transcripts from the ectopic vectors (Macias et al., 1996) encoding these six genes. The average number of aligned reads (± standard deviation) for the dataset was $2.9 \times 10^{7} \pm 1.3 \times 10^{7}$. Mapped reads were used to calculate TPMs using the software RSEM v1.2.3 (Li and Dewey, 2011). TPMs calculated by RSEM for non-mitochondrial transcripts were renormalized to a scale of one million non-mitochondrial transcripts before any further analysis. The software R v3.0.2 was employed either for principal component analysis (PCA) using the packages prcomp and scatterplot3d or for hierarchal clustering using hclust (with “complete” algorithm) and heatmap.2. The package heatmap.2 was also used to generate the heatmap for Figure S3A. The genes presented in Figure S3A were chosen from lists provided by AmiGO 2 (http://amigo.geneontology.org/amigo/landing) for Mus musculus using the terms “mesoderm development” (GO:0007498) “mesoderm formation” (GO:0001707), and “mesoderm morphogenesis” (GO:0048332). The PCA was performed on the $\log_2$(TPM) values of all genes whose expression was greater than two TPM for at least one replicate. A description of principle component analysis can be found elsewhere (Ringner, 2008). The hierarchal clustering was performed on the Spearman correlations between samples, using only genes whose expression was greater than eight TPM for at least one sample, with a $\log_2$ fold ratio greater than two between the highest and lowest expressers. In hierarchical clustering, the lengths of the branches are qualitatively proportional to the difference between samples. The GEO accession number for the RNA-seq data reported in this paper is GSE60896.

Cell imaging

Time lapse and single images were taken on a BioStation CT microscope (Nikon) and analyzed using CL Quant software version 3.00. Time-lapse images were converted into QuickTime movie files using ImageJ software version 1.43u, 50% image scaling, five frames per second, Sorenson

compression, and maximum quality. ImageJ is freely available at http://rsbweb.nih.gov/ij/. ImageJ software was used to convert TIFF images into JPEG images using default settings, except for Figure S1J, in which the brightness and contrast of the images was adjusted for visualization upon reduction in size by changing the minimum and maximum displayed values to 35 and 115 respectively. Single images were also taken on an Evos FL Auto microscope using software revision 23486 and 26049 or on a Zeiss Axio Scope.A1 using iVision-Mac software V4.5.0 (BioVision Technologies). Single slice, fluorescent, confocal images were taken on a Nikon Eclipse Ti inverted microscope configured with Nikon A1R Confocal and analyzed using NIS-Elements C software V4.20.00 (Build 967).

Other software used
The software Mstat version 5.5.1 (N. Drinkwater, University of Wisconsin) was employed for statistical analysis. It is freely available at http://www.mcardle.wisc.edu/mstat. To generate figures and text, the following software packages were used: Microsoft Word, Excel, and Powerpoint for Mac v14.3.6 – v14.4.4; Adobe Illustrator CSS v15.0.0 – v15.0.2; Endnote vX7.0.1; and Prism 6 for Mac v6.0c.

SUPPLEMENTAL REFERENCES

Barrett, S.D., Bridges, A.J., Dudley, D.T., Saltiel, A.R., Fergus, J.H., Flamme, C.M., Delaney, A.M., Kaufman, M., LePage, S., Leopold, W.R.*, et al.* (2008). The discovery of the benzhydroxamate MEK inhibitors CI-1040 and PD 0325901. Bioorganic & Medicinal Chemistry Letters *18*, 6501-6504.

Bryja, V., Bonilla, S., and Arenas, E. (2006). Derivation of mouse embryonic stem cells. Nature Protocols *1*, 2082-2087.

Chiang, P.M., and Wong, P.C. (2011). Differentiation of an embryonic stem cell to hemogenic endothelium by defined factors: essential role of bone morphogenetic protein 4. Development *138*, 2833-2843.

Choi, K.D., Vodyanik, M., and Slukvin, II (2011). Hematopoietic differentiation and production of mature myeloid cells from human pluripotent stem cells. Nature Protocols *6*, 296-313.

Chu, L.F., Surani, M.A., Jaenisch, R., and Zwaka, T.P. (2011). Blimp1 expression predicts embryonic stem cell development in vitro. Current Biology : CB *21*, 1759-1765.

Favata, M.F., Horiuchi, K.Y., Manos, E.J., Daulerio, A.J., Stradley, D.A., Feeser, W.S., Van Dyk, D.E., Pitts, W.J., Earl, R.A., Hobbs, F.*, et al.* (1998). Identification of a novel inhibitor of mitogen-activated protein kinase kinase. The Journal of Biological Chemistry *273*, 18623-18632.

Gharbi, S.I., Zvelebil, M.J., Shuttleworth, S.J., Hancox, T., Saghir, N., Timms, J.F., and Waterfield, M.D. (2007). Exploring the specificity of the PI3K family inhibitor LY294002. The Biochemical Journal *404*, 15-21.

Kent, D.G., Copley, M.R., Benz, C., Wohrer, S., Dykstra, B.J., Ma, E., Cheyne, J., Zhao, Y., Bowie, M.B., Gasparetto, M.*, et al.* (2009). Prospective isolation and molecular characterization of hematopoietic stem cells with durable self-renewal potential. Blood *113*, 6342-6350.

Langmead, B., Trapnell, C., Pop, M., and Salzberg, S.L. (2009). Ultrafast and memory-efficient alignment of short DNA sequences to the human genome. Genome Biology *10*, R25.

Li, B., and Dewey, C.N. (2011). RSEM: accurate transcript quantification from RNA-Seq data with or without a reference genome. BMC Bioinformatics *12*, 323.

Macias, M.P., Huang, L., Lashmit, P.E., and Stinski, M.F. (1996). Cellular or viral protein binding to a cytomegalovirus promoter transcription initiation site: effects on transcription. Journal of Virology *70*, 3628-3635.

Mohammadi, M., Froum, S., Hamby, J.M., Schroeder, M.C., Panek, R.L., Lu, G.H., Eliseenkova, A.V., Green, D., Schlessinger, J., and Hubbard, S.R. (1998). Crystal structure of an angiogenesis inhibitor bound to the FGF receptor tyrosine kinase domain. The EMBO Journal *17*, 5896-5904.

Morgan, K., Kharas, M., Dzierzak, E., and Gilliland, D.G. (2008). Isolation of early hematopoietic stem cells from murine yolk sac and AGM. Journal of visualized experiments : JoVE.

Pathak, G.K., Aranda-Espinoza, H., and Shah, S.B. (2014). Mouse hippocampal explant culture system to study isolated axons. Journal of Neuroscience Methods *232*, 157-164.

Ringner, M. (2008). What is principal component analysis? Nature Biotechnology *26*, 303-304.

Ruiz-Herguido, C., Guiu, J., D'Altri, T., Ingles-Esteve, J., Dzierzak, E., Espinosa, L., and Bigas, A. (2012). Hematopoietic stem cell development requires transient Wnt/beta-catenin activity. The Journal of Experimental Medicine *209*, 1457-1468.

Rybtsov, S., Sobiesiak, M., Taoudi, S., Souilhol, C., Senserrich, J., Liakhovitskaia, A., Ivanovs, A., Frampton, J., Zhao, S., and Medvinsky, A. (2011). Hierarchical organization and early hematopoietic specification of the developing HSC lineage in the AGM region. The Journal of Experimental Medicine *208*, 1305-1315.

Sargent, C.Y., Berguig, G.Y., and McDevitt, T.C. (2009). Cardiomyogenic differentiation of embryoid bodies is promoted by rotary orbital suspension culture. Tissue Engineering Part A *15*, 331-342.

Sturgeon, C.M., Chicha, L., Ditadi, A., Zhou, Q., McGrath, K.E., Palis, J., Hammond, S.M., Wang, S., Olson, E.N., and Keller, G. (2012). Primitive erythropoiesis is regulated by miR-126 via nonhematopoietic Vcam-1+ cells. Developmental Cell *23*, 45-57.

Taoudi, S., Gonneau, C., Moore, K., Sheridan, J.M., Blackburn, C.C., Taylor, E., and Medvinsky, A. (2008). Extensive hematopoietic stem cell generation in the AGM region via maturation of VE-cadherin+CD45+ pre-definitive HSCs. Cell Stem Cell *3*, 99-108.

Xiao, Q., Zeng, L., Zhang, Z., Hu, Y., and Xu, Q. (2007). Stem cell-derived Sca-1+ progenitors differentiate into smooth muscle cells, which is mediated by collagen IV-integrin alpha1/beta1/alphav and PDGF receptor pathways. American Journal of Physiology Cell Physiology *292*, C342-352.

Xie, W., Schultz, M.D., Lister, R., Hou, Z., Rajagopal, N., Ray, P., Whitaker, J.W., Tian, S., Hawkins, R.D., Leung, D.*, et al.* (2013). Epigenomic analysis of multilineage differentiation of human embryonic stem cells. Cell *153*, 1134-1148.

Yusa, K., Zhou, L., Li, M.A., Bradley, A., and Craig, N.L. (2011). A hyperactive piggyBac transposase for mammalian applications. Proceedings of the National Academy of Sciences of the United States of America *108*, 1531-1536.

Zhang, J., Liu, J., Huang, Y., Chang, J.Y., Liu, L., McKeehan, W.L., Martin, J.F., and Wang, F. (2012). FRS2alpha-mediated FGF signals suppress premature differentiation of cardiac stem cells through regulating autophagy activity. Circulation Research *110*, e29-39.